Development of new non-viral systems for genetic modification of senescent cells

Junquera López-Seijas,[1,3] Diego Miranda-Balbuena,[1,3] Alba Iglesias-Fente,[1] Marta Sacristán-Santos,[1] Natalia Carballo-Pedrares,[1] María C. Arufe,[2] Ana Rey-Rico,[1] and Juan Fafián-Labora[2]

[1]Gene and Cell Therapy Research Group (G-CEL), Centro Interdisciplinar de Química e Bioloxía - CICA, Universidade da Coruña, 15071 A Coruña, Spain; [2]Departamento de Fisioterapia, Medicina y Ciencias Biomédicas, Facultad de Ciencias de la Salud, Universidade da Coruña (UDC), Instituto de Investigación Biomédica de A Coruña (INIBIC), Complexo Hospitalario Universitario de A Coruña (CHUAC), Servizo Galego de Saúde (SERGAS), 15006 A Coruña, Spain. Centro Interdisciplinar de Química e Bioloxía - CICA, Universidade da Coruña, 15071 A Coruña, Spain

Senescence is a process characterized by a prolonged irreversible cell-cycle arrest. The accumulation of senescent cells in tissues is related to aging and to the development of age-related diseases. Recently, gene therapy has emerged as a powerful tool for treating age-associated diseases by the transference of specific genes into the target cell population. However, the high sensitivity of senescent cells significantly precludes their genetic modification via classical viral and non-viral systems. Niosomes are self-assembled non-viral nanocarriers that exhibit important advantages due to their elevated cytocompatibility, versatility, and cost-efficiency, arising as a new alternative for genetic modification of senescent cells. In this work, we explore for the first time the use of niosomes for genetic modification of senescent umbilical cord-derived mesenchymal stem cells. We report that niosome composition greatly affected transfection efficiency; those formulations prepared in medium with sucrose and containing cholesterol as helper lipid being the most suitable to transfect senescent cells. Moreover, resulting niosome formulations exhibited a superior transfection efficiency with a markedly less cytotoxicity than the commercial reagent Lipofectamine. These findings highlight the potentiality of niosomes as effective vectors for genetic modification of senescent cells, providing new tools for the prevention and/or treatment of age-related diseases.

INTRODUCTION

Aging is a complex process that progressively compromises most of the biological functions from organisms, resulting in an increased susceptibility to disease and death.[1] Therefore, aging depicts a major risk factor in many human diseases such as fibrosis, osteoarthritis,[2] dementia,[3] glaucoma,[4] cancer,[5] and type 2 diabetes.[6]

Senescence is a cellular response attributed to a stable cycle arrest and plays physiological roles during normal development. However, senescence also forms a stress response triggered by hallmarks associated with aging.[7]

Cell-based therapies are promising options for the treatment of several degenerative diseases related to aging such as osteoarthritis,[8]

Parkinson's,[9] and retinal diseases.[10] Specifically, mesenchymal stem cells (MSCs) represent the ideal cell population for the treatment of age-related diseases[11] due to their undifferentiated nature, high proliferation and differentiation capacity, and immunomodulatory properties.[12] However, there are limitations of stem cell-based therapies such as poor long-term maintenance of stem cell function.[13,14]

Similar to normal somatic cells, adult MSCs are exposed to stressors during their lifespan, leading to an age-dependent decline in their number that results in the impairment of tissue homeostasis, regeneration, and repair.[15] Aging of the MSC niche causes spontaneously inflammatory responses and interferes with the effect of MSC-based therapy.[16] Hence, MSC senescence is directly related to the development of age-related diseases such as osteoarthritis, osteoporosis, and frailty.[17]

The development of anti-aging therapies to preserve native properties of MSCs or even revert their senescent phenotype has gained special significance in last decades. Particularly, senolytic drugs constitute the first-line treatment to selectively kill and decrease the accumulation of senescent cells in several tissues and organs related to aging, exhibiting benefits in the treatment of several age-related pathologies such as type 2 diabetes, Alzheimer's disease, or atherosclerosis.[18] However, they are unspecific and can produce side effects.[19,20]

Gene therapy applied to MSCs has emerged as a promising tool for the treatment of several pathologies including those related to

aging.[21–23] Current gene transfer vectors to genetically modify MSCs include viral and non-viral vectors. Viral vectors, because they rely on the natural properties of viruses to introduce genetic material into cells, constitute the most widespread tool due to their high efficiency of genetic modification. However, their use is associated with a series of important limitations such as the risk of oncogenesis, high immunogenicity, and/or activation of inflammatory pathways that reduce their potential for the development of therapies aimed at the treatment of diseases associated with aging.[1,24] Thus, non-viral vectors have gained special attention due to their high biosafety, low production costs, and ease of manipulation. Still, and despite their potential advantages, non-viral vectors exhibit a reduced transfection efficiency when compared with their viral counterparts.[25] Liposomes represent the most widely used systems in gene therapy assays both *in vitro* and *in vivo*.[26] Although the gene transfer efficiency of liposomes has been implemented in recent years, their high intrinsic toxicity, mostly when working with primary cells, strongly limit their use, highlighting the need to search for alternative systems.

Niosomes are liposome-like nanovesicles consisting of cationic lipids, non-ionic surfactants, and helper lipids that have recently arisen as promising non-viral gene delivery systems.[27–29] The presence of non-ionic surfactants in their structure instead of phospholipids, as in the case of liposomes, provides these systems with greater charge stability, as well as notably lower toxicity and production costs.[30] Niosomes have been formulated by combination of cationic lipids (e.g., 1,2-di-O-octadecenyl-3-trimethylammonium propane [DOTMA], DOPA)[31–33] with non-ionic surfactants including polysorbate 20 (P20),[34,35] polysorbate 60 (P60),[31,36,37] or polysorbate 80 (P80).[34,38,39] Moreover, the effect of the addition of various helper lipids as squalene (SQ),[27,28,35,37,39–43] cholesterol (CH),[44] or lycopene[31,36,37] to niosome systems has been also investigated. While most of these niosome formulations have been tested to target the central nervous system or retina cells, only a few studies have explored the suitability to these systems to genetically modify MSCs.[24,29,31] Of note, none of these studies has explored the possibility of targeting MSCs with senescent phenotype.

The heterogeneous morphology, high sensitivity, and persistent activation of inflammatory pathways,[45] characteristic of senescent cells, significantly preclude their genetic modification using conventional vectors.[46] This fact urges the need of using alternative carriers for genetically modifying cells with a senescent phenotype. We previously formulated niosome suspensions based on the combination of the cationic lipid DOTMA with the non-ionic surfactants P60[24] or a blend of P80 with poloxamer 407 (PX)[43] with the helper lipids SQ[43] or CH[24] to transfect MSCs. Of note, some of the developed formulations led to similar values of transfection to those achieved with the commercial reagent Lipofectamine (LPF).[24,43] Moreover, incorporation of the lysosomotrophic agent sucrose to the niosome formulations significantly increased the transfection efficiency.[24]

Based on this, the aim of this work was to explore, for the first time to the best of our knowledge, the possibility of using non-viral systems based on niosomes for the genetic modification of senescent MSCs.

Two niosome formulations were produced by fixing the content of the cationic lipid DOTMA and non-ionic surfactants (P20 and PX) and varying the composition of the helper lipid (SQ or CH). Resulting nioplexes from complexation of niosomes with the reporter plasmid pEGFP were characterized in terms of size, polydispersity index (PDI), charge distribution, capacity of DNA protection, and complexation ability. Furthermore, GFP transfection efficiency and cytotoxic profiles of nioplexes were studied in primary cultures of non-senescent and senescent UC-MSCs isolated from samples of two different patients. Next, the addition of the lysosomotropic agent sucrose to the niosome dispersions was explored as a way to enhance the performance of the developed gene delivery systems.[24] Finally, the endocytic pathways in non-senescent and senescent UC-MSCs of the most suited nioplex formulations were explored.

RESULTS

Isolation and establishment of an UC-MSC senescence model

To elucidate the potential of niosome formulations as gene carriers to genetically modify senescent cells, a model of senescence in MSCs isolated from the umbilical cord (UC) was stablished. For that, UC-MSCs were firstly characterized by the expression of mesenchymal and hematopoietic markers using flow cytometry.

Resulting isolated UC-MSCs showed percentages of positivity of mesoderm markers (CD90, CD73, and CD105) higher than 56% (Figure S1). Conversely, the expression of hematopoietic markers (CD34 and CD45) was lower than 1%. In addition, the expression of undifferentiated markers (*NANOG*, *SOX2*, *OCT3/4*, and *REX1*) in UC-MSCs was studied at the mRNA level and compared with that obtained in the healthy chondrocyte cell line TC28a2. Expression of these markers was significantly higher in UC-MSCs when compared with healthy chondrocytes (p < 0.01) (Figure S2) these last ones exhibiting values close to 0.

Once characterized, we established a therapy-induced senescence (TIS) model of UC-MSCs. To this end, cells were treated for 6 days with Palbociclib, a selective inhibitor of cyclin-dependent kinase 4 and 6 (CDK4/6)[47] (Figure S3A). A marked reduction in proliferation of senescent UC-MSCs was demonstrated using crystal violet staining (Figure S3B). Likewise, when analyzing cell morphology by optical microscopy, senescent UC-MSCs were flatter and bigger than non-senescent cells (Figure S3C).

To further confirm the senescent phenotype of UC-MSCs, the expression of the endogenous markers of cell-cycle arrest such as CDK inhibitors (*CDKN1A* and *CDKN2A*) and markers related to the senescence-associated secretory phenotype (SASP) such as interleukin-6 and -8 (*IL-6* and *IL-8*) was monitored by quantitative reverse-transcription PCR (qRT-PCR). Expression of *CDKN1A*, *IL-8*, and *IL-6* was increased by 435.3-, 74.0-, and 134.4-fold in senescent cells compared with non-senescent cells (p ≤ 0.03) (Figure S3D).

Physicochemical characterization of niosomes and nioplexes

Niosomes were prepared using the reversed-phase evaporation method and characterized in terms of particle size, PDI, and
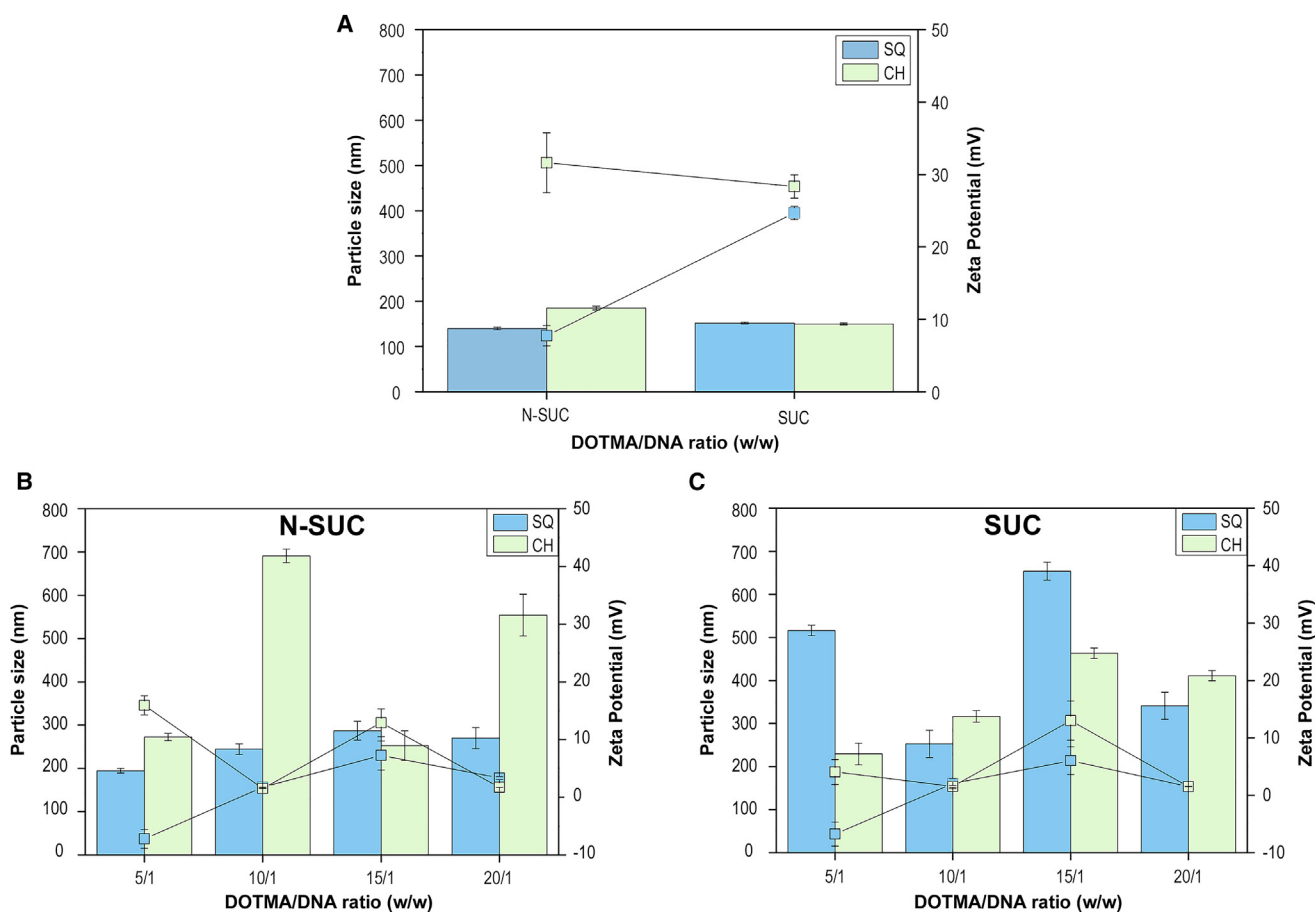
Figure 1. Physicochemical features of niosomes and nioplexes

Particle size and Z potential of squalene (SQ) and cholesterol (CH) niosomes prepared in the absence (N-SUC) or presence (SUC) of sucrose (A) and their respective complexes after complexation with pEGFP (700 ng) at DOTMA/DNA ratios of 5/1, 10/1, 15/1, and 20/1, respectively (B and C). Data are shown as mean ± SD.

superficial charge. Figure 1A depicts the size and Z potential values measured for SQ and CH niosome formulations. Niosomes formulated with CH were significantly larger ($\sim$185 nm) than those formulated with SQ ($\sim$140 nm) ($p < 0.001$) (Figure S4). Likewise, a significantly higher electropositivity was demonstrated in niosomes formulated with CH ($\sim$23 mV) compared with those comprised of SQ ($\sim$7.7 mV) ($p < 0.001$). Niosome formulations prepared in medium with sucrose were also characterized (Figure 1A). In contrast to niosomes prepared in the absence of sucrose, no differences were observed in the size from SQ or CH formulations ($p = 0.862$) (Figure S4). A similar trend was observed when measuring Z potential, showing comparable values of electropositivity ($\sim$26 mV) ($p = 0.256$).

Nioplexes were formed upon complexation of pEGFP with SQ and CH niosomes at DOTMA/DNA ratios (w/w) of 5/1, 10/1, 15/1, and 20/1. The size of CH nioplexes was always higher than that measured for SQ complexes at 5/1, 10/1, and 20/1 DOTMA/DNA ratios ($p < 0.001$) in the absence of sucrose (Figure 1B). The incorporation of sucrose to niosome formulations caused a significant increment in

size of SQ complexes at DOTMA/DNA ratios of 5/1, 15/1, and 20/1 ($p < 0.001$) and at a 15/1 ratio of CH formulations ($p < 0.001$) (Figure 1C). With respect to Z potential, SQ formulations showed a tendency to a higher electropositivity by increasing their DOTMA/DNA ratios from 5/1 to 10/1 followed by a reduction of the electropositivity from 15/1 to 20/1 ($p < 0.006$). In contrast, CH formulations showed higher electropositivity at 5/1 and 15/1 DOTMA/DNA ratios and the lowest ones at 10/1 and 20/1 (Figure 1B). Same tendencies were reached when sucrose was added into the medium of both formulations (Figure 1C). Focusing on PDI values, both niosome formulations exhibited a similar tendency, with stable values of $\sim$0.33 ($p > 0.151$). Beyond, these values were slightly higher when DNA was complexed in CH nioplexes but lower in SQ nioplexes ($\sim$0.36 for CH and $\sim$0.28 for SQ complexes). However, in the presence of sucrose, PDI values were decreased in CH nioplexes but increased in SQ formulations (Table S1).

Agarose gel electrophoresis assay in the presence of DNase I was performed with nioplexes formed with SQ and CH niosome formulations at 5/1, 10/1, 15/1, and 20/1 DOTMA/DNA ratios (Figure 2A).
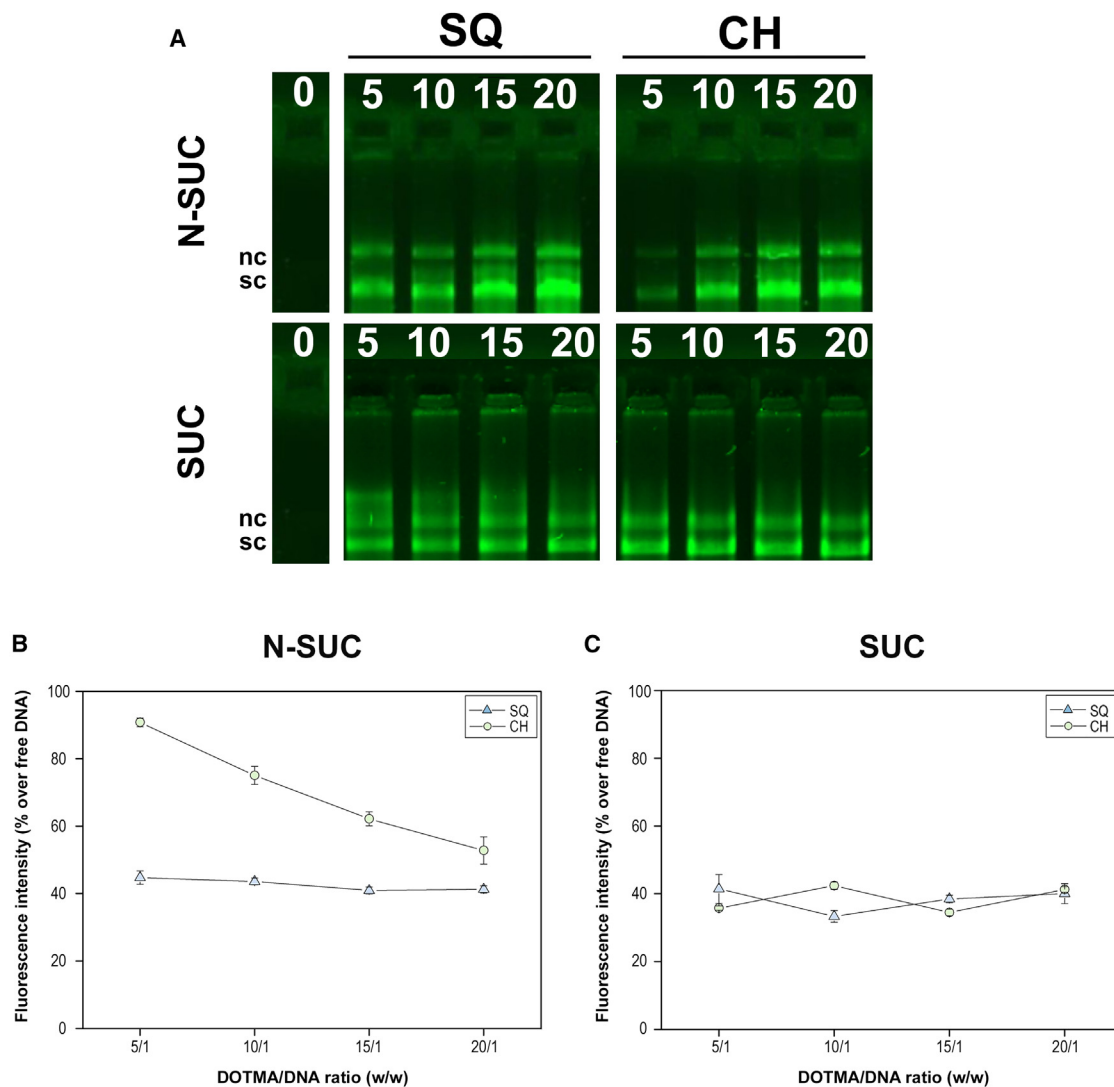
Figure 2. Protection and complexation abilities of niosomes

DNase I protection ability and SDS-induced release visualized by agarose electrophoresis of squalene (SQ) and cholesterol (CH) nioplexes formed at DOTMA/DNA ratios of 5/1, 10/1, 15/1, and 20/1 prepared in the absence (N-SUC) or presence (SUC) of sucrose. 0, naked pEGFP; NC, nicked circular; SC, supercoiled (A). DNA complexation efficiency of squalene (SQ) and cholesterol (CH) nioplexes formed at DOTMA/DNA ratios of 5/1, 10/1, 15/1, and 20/1 prepared in the absence (N-SUC) (B) or presence (SUC) of sucrose (C). Data are shown as mean ± SD.

Both SQ and CH formulations protected DNA from DNase I digestion, as confirmed by the presence of bands corresponding to supercoiled (SC) and nicked circular (NC) DNA forms at all DOTMA/DNA ratios tested (Figure 2A). Of note, a progressive increment of SC band intensities was demonstrated when increasing the DOTMA/DNA ratio for both formulations. Moreover, SQ formulations showed higher capacity of protection than CH ones at the lowest DOTMA/DNA ratio tested (5/1).

Complexation of DNA with the niosome formulations

A fluorophore exclusion assay was performed to evaluate the ability of SQ and CH niosome formulations to efficiently condense DNA (Figure 2B). Irrespective of the DOTMA/DNA ratio considered, the ability of complexation of SQ niosomes was marked higher than those comprising CH, when formulations were prepared without sucrose ($p < 0.004$). Moreover, only CH formulations showed a tendency to a higher condensation when increasing the DOTMA/DNA ratio ($p < 0.001$ when comparing nioplexes formed at 5/1 with those formed at 20/1 DOTMA/DNA ratio).

The incorporation of sucrose in CH formulations led to a significant increment in their ability to complex DNA ($p < 0.001$) (Figure 2C). In contrast, not statistically significant differences were observed when sucrose was incorporated into SQ formulations ($p > 0.053$).
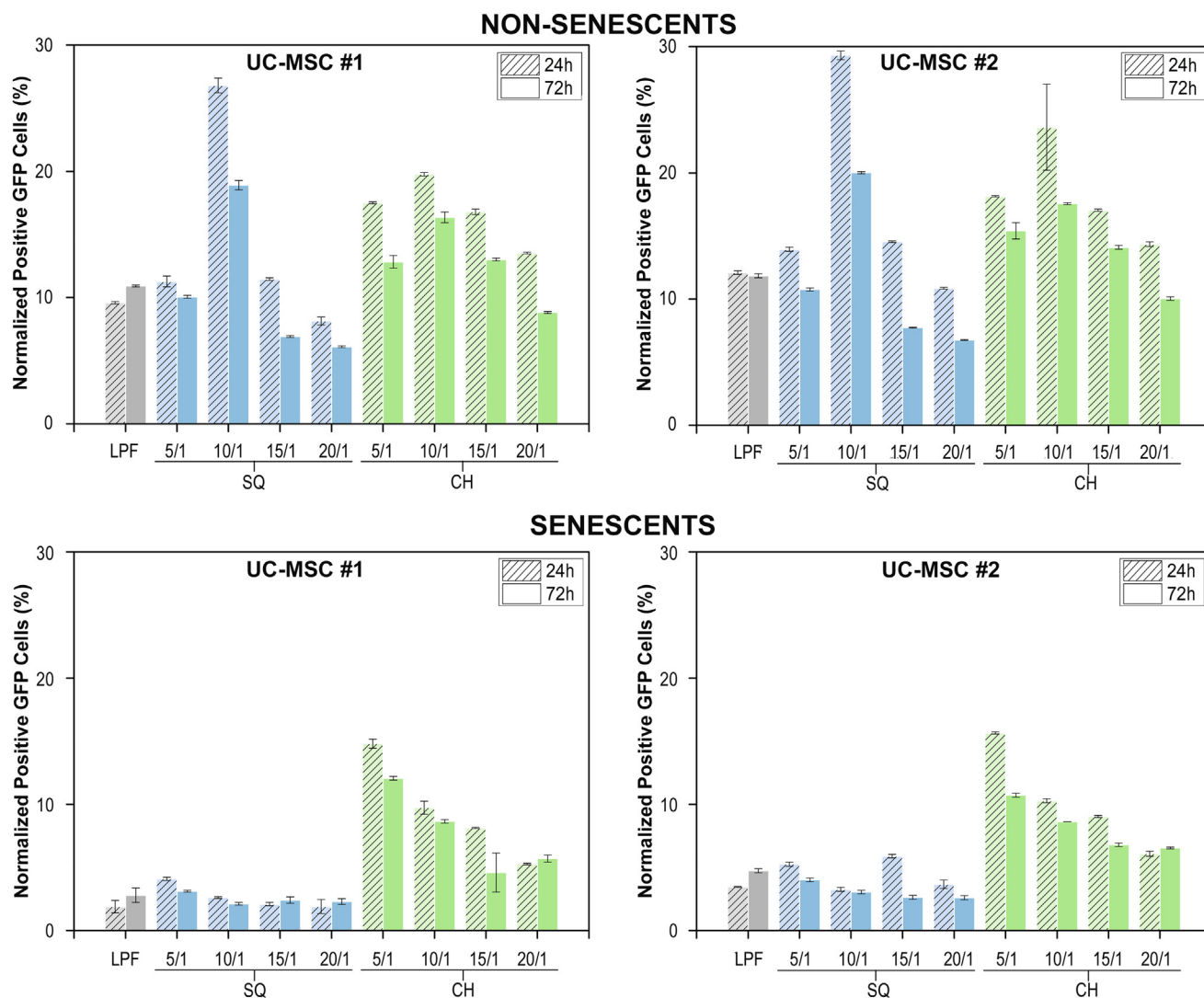
Figure 3. Transfection efficiency of nioplexes

GFP transgene expression (%) in non-senescent (upper panels) and senescent (lower panels) UC-MSCs isolated from patients no. 1 (left) and no. 2 (right) transfected with Lipofectamine (LPF) or with niosome formulations of squalene (SQ) or cholesterol (CH) at DOTMA/DNA ratios of 5/1, 10/1, 15/1, and 20/1 at 24 and 72 h. Data are shown as mean ± SD.

In vitro transfection efficiency of UC-MSCs using niosome formulations

The transfection efficiency of SQ and CH nioplexes was evaluated at 24 and 72 h of contact with monolayer cultures of non-senescent and senescent UC-MSCs isolated from two different patients (nos. 1 and 2) by flow cytometry (Figure 3).

Irrespective of the formulation considered, transfection efficiencies of non-senescent UC-MSC no. 1 were always higher at 24 h compared with 72 h, as shown by the absence of an interaction between both factors (formulation type and time point) ($p = 0.457$) (Figure 3, upper panels). A similar trend was observed in non-senescent UC-MSC

no. 2, although an interaction between both factors was observed ($p < 0.001$) (Figure 3, lower panels).

Focusing on DOTMA/DNA ratios of nioplexes, the highest transfection efficiencies were reached at 24 h of contact with SQ niosomes formulated at 10/1 (∼28% GFP positivity; up to 3.3- and 2.7-fold difference compared with the rest of formulations in UC-MSC no. 1 and UC-MSC no. 2, respectively; $p < 0.001$). GFP expression percentages were significantly lower after 3 days ($p < 0.001$), those SQ nioplexes formulated at DOTMA/DNA ratio of 10/1 leading again to the highest efficiencies (∼20% GFP positivity; up to 3.1- and 3.0-fold difference compared with the rest of formulations in UC-MSC no. 1 and
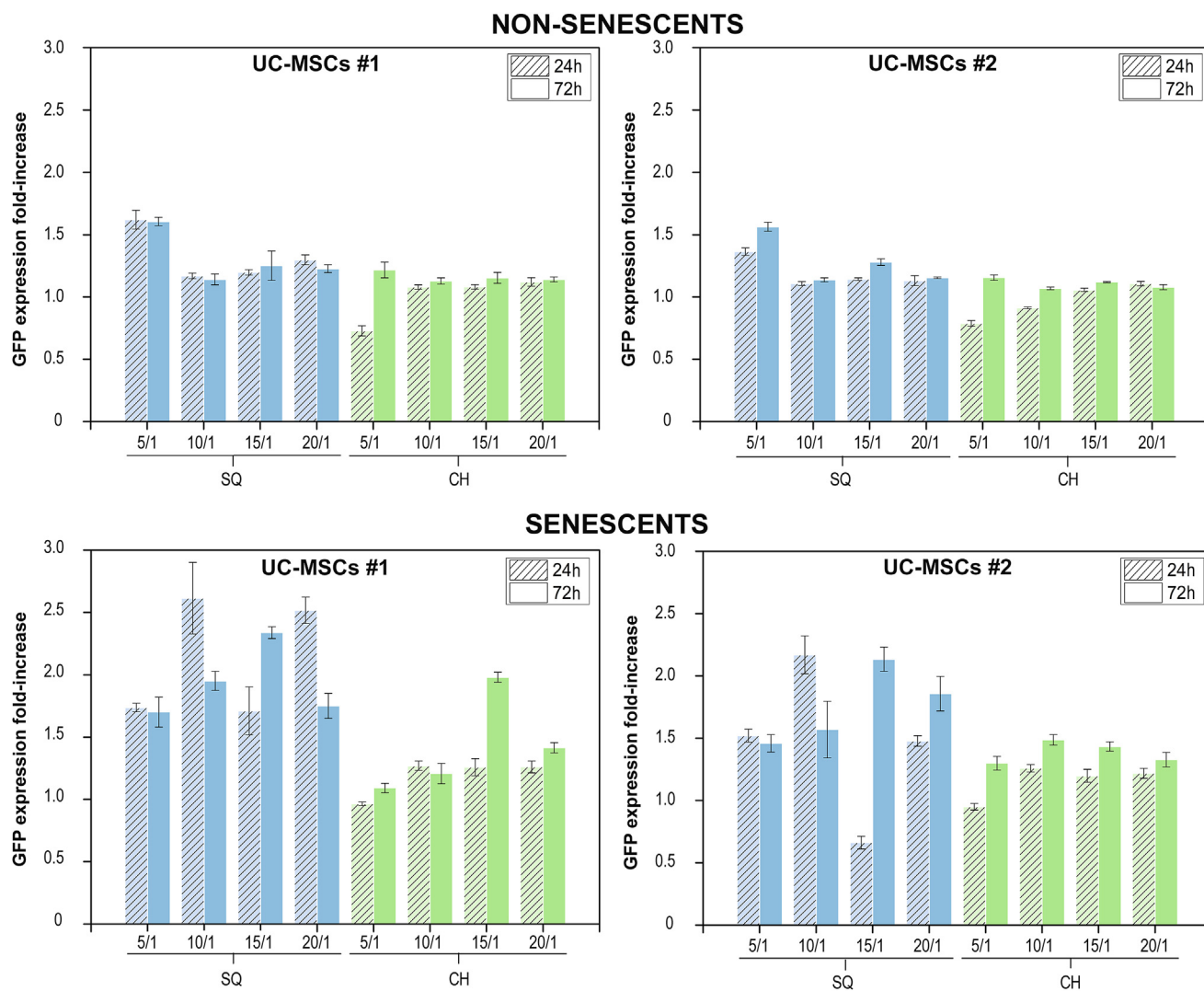
NON-SENESCENTS

SENESCENTS

Figure 4. Effect of sucrose on nioplexes transfection efficiency
GFP expression fold-increase of non-senescent (upper panels) and senescent (lower panels) UC-MSCs isolated from patients no. 1 (left) and no. 2 (right) transfected with niosome formulations of squalene (SQ) or cholesterol (CH) at DOTMA/DNA ratios of 5/1, 10/1, 15/1, and 20/1 prepared in medium containing sucrose relative to same formulations prepared in medium without sucrose. Data are shown as mean ± SD.

UC-MSC no. 2, respectively; $p < 0.001$). Of note, transfection efficiencies reached with SQ nioplexes at 10/1 DOTMA/DNA ratio were significantly higher than those achieved with the commercial reagent LPF (up to 2.80- and 2.40-fold increase at 24 h of contact with UC-MSC no. 1 and UC-MSC no. 2, respectively; $p < 0.001$).

Similar to that observed in non-senescent cells, transfection of senescent UC-MSCs via SQ or CH niosome formulations led to the highest efficiencies after 24 h of contact ($p < 0.001$). In contrast, the highest GFP transfection efficiencies were reached with CH nioplexes at a DOTMA/DNA ratio of 5/1 (∼15% GFP positivity; up to 7.80-fold in UC-MSC no. 1 and up to 4.80-fold in UC-MSC no. 2 when compared with the rest of formulations at 24 h of contact;

$p < 0.001$). Of note, the levels of GFP transgene expression when using CH niosomes were significantly higher than those achieved with SQ formulations at all DNA ratios tested ($p < 0.001$). Likewise, these levels were significantly greater than those achieved with LPF (up to 7.8- and 4.5-fold difference in UC-MSC no. 1 and UC-MSC no. 2, respectively; $p < 0.001$). Moreover, when focusing on CH formulations an inverse relationship on transfection efficiency was demonstrated by raising the DOTMA/DNA ratio from 5/1 (∼15% GFP positivity) to 20/1 (∼6% GFP positivity; $p < 0.001$).

In a next step, transfection experiments in non-senescent and senescent UC-MSCs were repeated using niosome dispersions re-suspended in medium containing sucrose to elucidate whether the
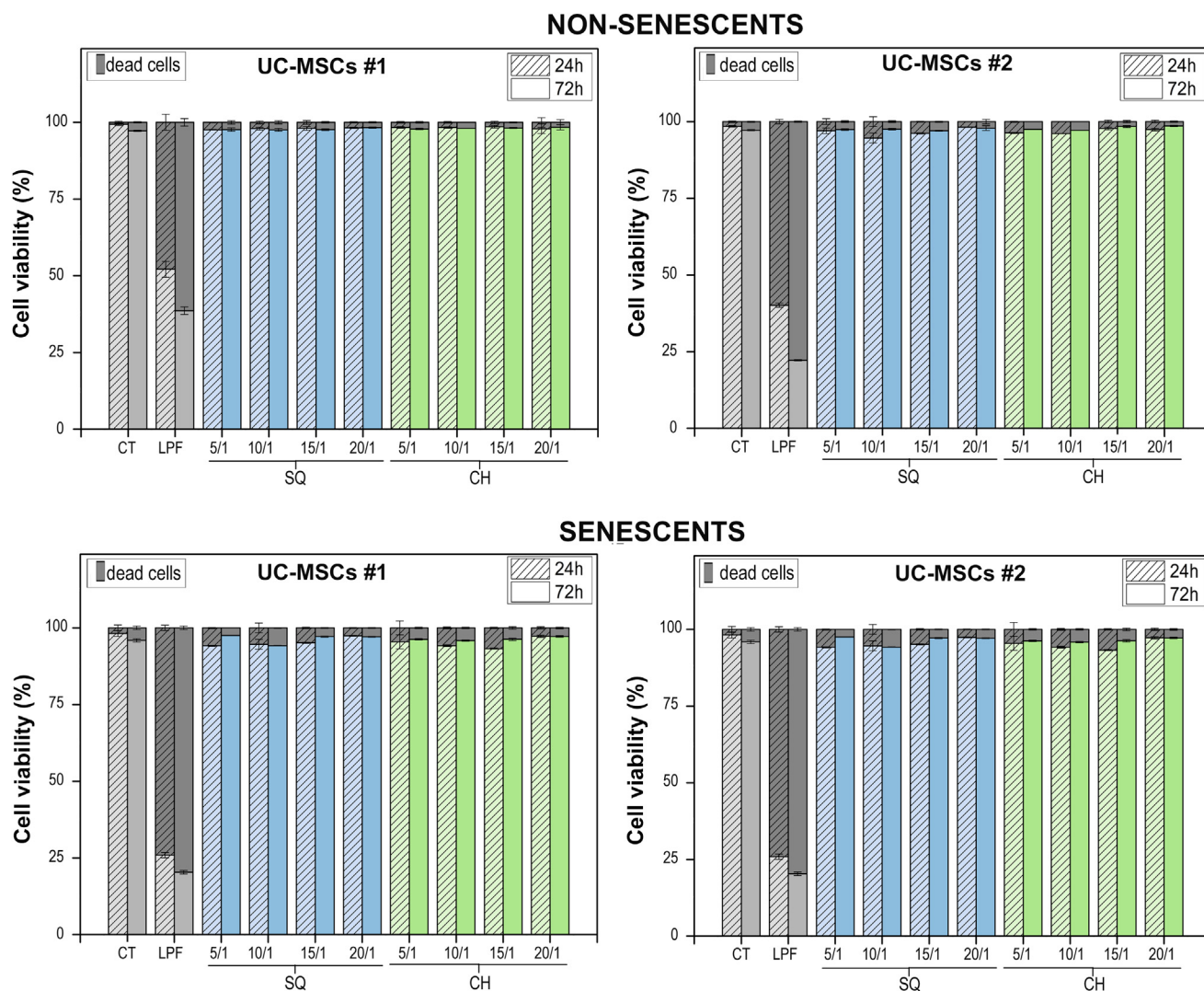
Figure 5. Cytotoxic profile of nioplexes

Cell viability percentages of non-senescent (upper panels) and senescent (lower panels) UC-MSCs isolated from patients no. 1 (left) and no. 2 (right) untransfected (control; CT) or transfected using niosome formulations of squalene (SQ) or cholesterol (CH) at DOTMA/DNA ratios of 5/1, 10/1, 15/1, and 20/1 or Lipofectamine (LPF) at 24 and 72 h. Gray stacked bars denote cytotoxicity percentages in the presence of same compounds. Data are shown as mean ± SD.

transfection efficiency of nioplexes may be enhanced due to a favored endosomal escape[24] (Figure 4).

Incorporation of sucrose to SQ niosome formulations significantly increased the transfection efficiency of non-senescent cells at all ratios and time points studied (up to 1.6-fold in UC-MSC no. 1 and UC-MSC no. 2 at 24 and 72 h of contact, respectively; p < 0.001). In contrast, a more discrete effect was demonstrated upon addition of sucrose to CH niosome formulations (up to 1.2-fold difference in non-senescent UC-MSC no. 1 and MSC no. 2 at 72 h of contact; p < 0.001).

A significant increase in transfection efficiency of senescent cells was demonstrated at 24 h post-transfection using niosome dispersions prepared in sucrose at all ratios tested (always p ≤ 0.019), except those comprising CH at the lowest DOTMA/DNA ratio tested (5/1; p > 0.212). Incorporation of sucrose to SQ formulations led to the highest increments of GFP transgene expression at 24 h (up to 2.6-fold in UC-MSC no. 1 and up to 2.2-fold in UC-MSC no. 2 relative to formulations prepared in medium; p < 0.001). However, incorporation of sucrose to CH niosome dispersion led to the highest increases on transfection efficiency after 72 h of contact (up to 2.0- and 1.5-fold in UC-MSC no. 1 and UC-MSC no. 2, respectively relative to the same formulations prepared in medium; p ≤ 0.001).

To confirm the results obtained by flow cytometry, the transfection of MSCs after 24 h using SQ and CH nioplexes at 10/1 and 5/1
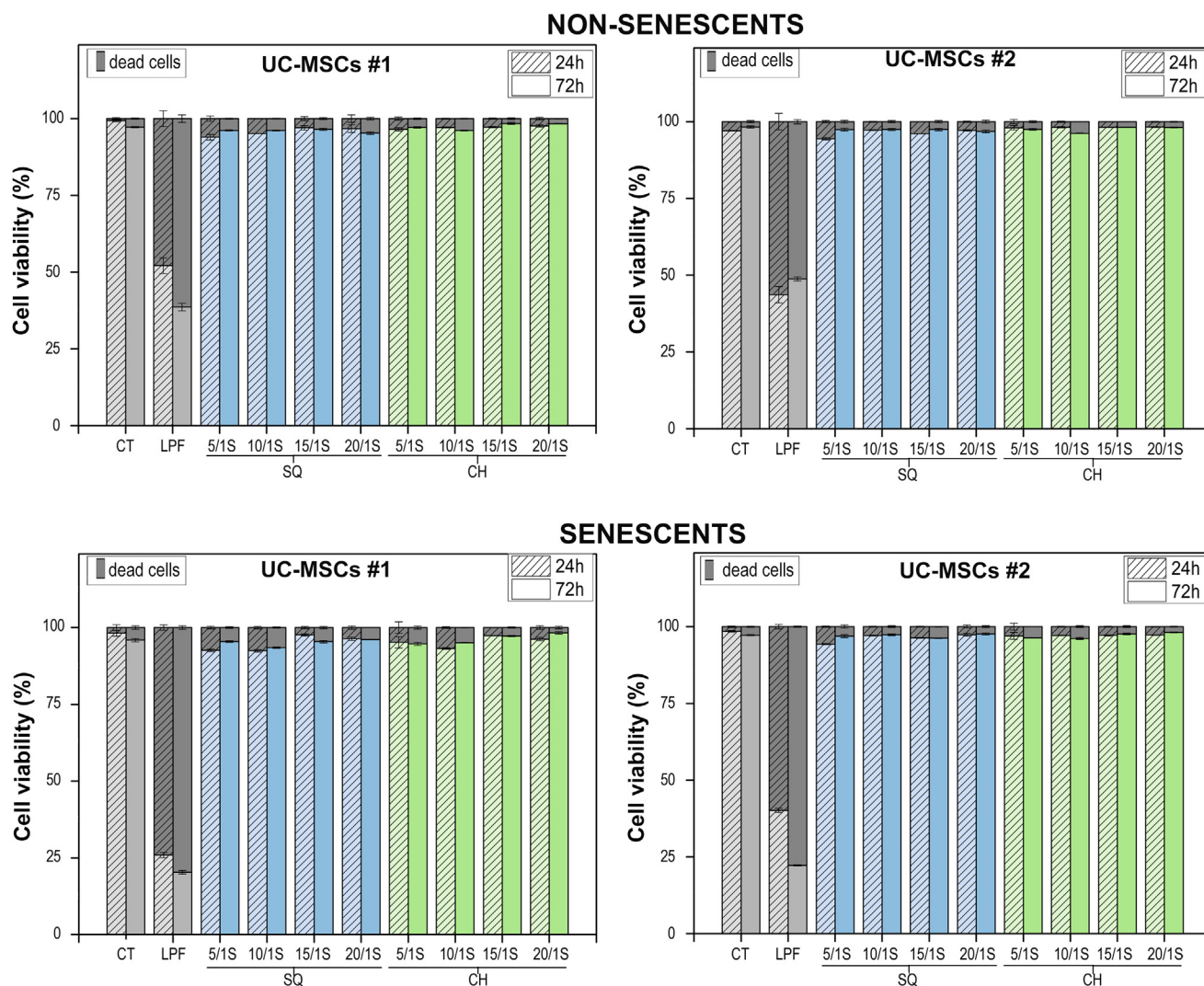
Figure 6. Effect of sucrose on nioplexes cytotoxic profile

Cell viability percentages of non-senescent (upper panels) and senescent (lower panels) UC-MSCs isolated from patients no. 1 (left) and no. 2 (right) untransfected (control; CT) or transfected using niosome formulations of squalene (SQ) or cholesterol (CH) prepared in the presence of sucrose (S) at DOTMA/DNA ratios of 5/1, 10/1, 15/1, and 20/1 or Lipofectamine (LPF) at 24 and 72 h. Gray stacked bars denote cytotoxicity percentages in the presence of same compounds. Data are shown as mean ± SD.

DOTMA/DNA ratios, respectively, in the absence (N-SUC) and presence (SUC) of sucrose, was evaluated under the Nikon Eclipse TI microscope (Nikon, Japan). The cells incorporated the DNA and expressed the GFP protein (Figure S5).

Cell viability of UC-MSCs upon transfection with niosome formulations

Cytotoxic profiles of SQ and CH nioplexes upon contact with non-senescent and senescent UC-MSC nos. 1 and 2 were evaluated at 24 and 72 h post-transfection by flow cytometry (Figures 5 and S6). No differences in live cells percentages were found in non-senescent UC-MSCs (Figure 5, upper panels) transfected with nioplexes compared with untransfected cells (control) at any of the time points

evaluated (viability $\geq$ 96%; $p \geq 0.262$). A similar trend was observed upon transfection of senescent cells (Figure 5, lower panels), with nioplexes always exhibiting cell survival percentages higher than 94% in both UC-MSC nos. 1 and 2, despite statistically significant differences being reached when compared with control untreated cells ($p < 0.05$). Conversely, a significant reduction in cell viability was demonstrated when UC-MSCs were transfected with LPF in both non-senescent (viability $\sim$45%; $p < 0.031$; Figure 5, upper panels) and senescent cells ($\sim$27%; $p < 0.005$; Figure 5, lower panels).

Cell viability upon transfection with niosome dispersions prepared in medium with sucrose was also evaluated (Figures 6 and S6). Similar to niosomes prepared in medium without sucrose, no cytotoxic effects
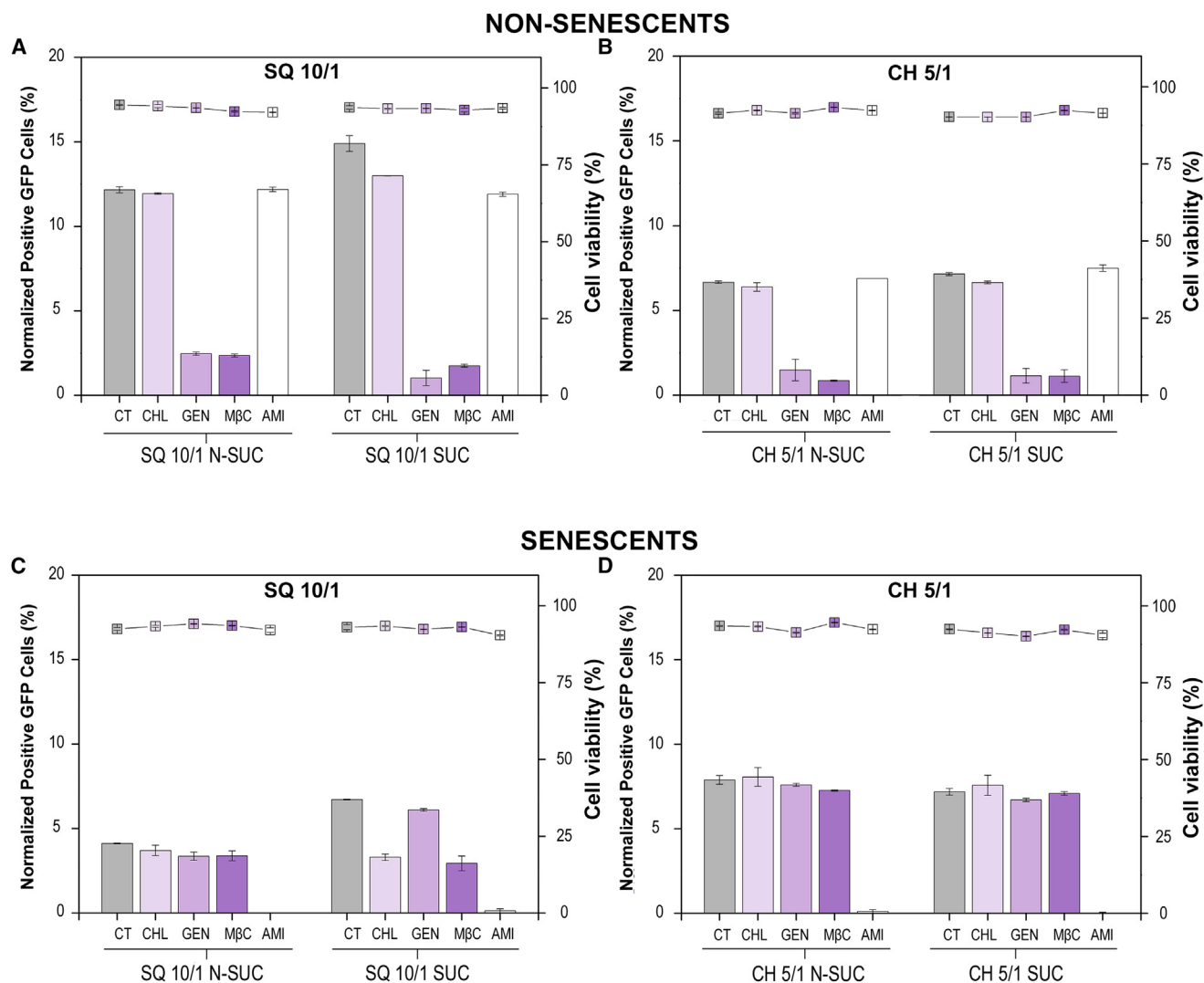
Figure 7. Effect of endocytosis inhibitors in GFP expression and cell viability

Normalized positive GFP expression percentages and cell viability percentages of non-senescent (A and B) or senescent (C and D) UC-MSCs preincubated with chlorpromazine (CHL), genistein (GEN), methyl-β-cyclodextrin (MβC), and amiloride (AMI) or not (control; CT) and transfected using niosome formulations of squalene (SQ) or cholesterol (CH) prepared in the absence (N-SUC) or presence (SUC) of sucrose at DOTMA/DNA ratios of 10/1 and 5/1, respectively. Data are shown as mean ± SD.

were observed upon transfection of UC-MSCs with niosomes prepared in sucrose in both non-senescent (viability ≥94%; Figure 6, upper panels) or senescent cells (viability ≥92%; Figure 6, lower panels) although statistically significant differences were reached when compared with control untreated cells ($p \geq 0.001$). Likewise, these percentages of cell survival were significantly higher than those achieved with LPF ($p < 0.005$).

The mechanism underlying the uptake of nioplexes into non-senescent and senescent UC-MSCs was investigated using the specific inhibitors for distinguishing endocytic pathways (Figures 7 and S7). A different uptake mechanism of selected nioplex formulations was observed according to cell phenotype. Incubation of non-senescent

cells with genistein or methyl-β-cyclodextrin significantly decreased transfection efficiency of SQ niosomes prepared in medium with or without sucrose at 10/1 DOTMA/DNA ratio ($p \leq 0.001$) (Figure 7A), implying that the entry of SQ nioplexes into non-senescent cells was through caveolae-mediated endocytosis. A similar trend was observed with CH nioplexes formed at 5/1 DOTMA/DNA ratio and cell pre-incubation with genistein or methyl-β-cyclodextrin leading to a significant reduction in GFP expression ($p \leq 0.001$) (Figure 7B).

In contrast, a significant reduction of GFP transgene expression was demonstrated upon pre-incubation of senescent cells with amiloride before transfection with SQ or CH nioplexes formed at 10/1 and 5/1 DOTMA/DNA ratios, respectively ($p \leq 0.001$) (Figures 7C and 7D,
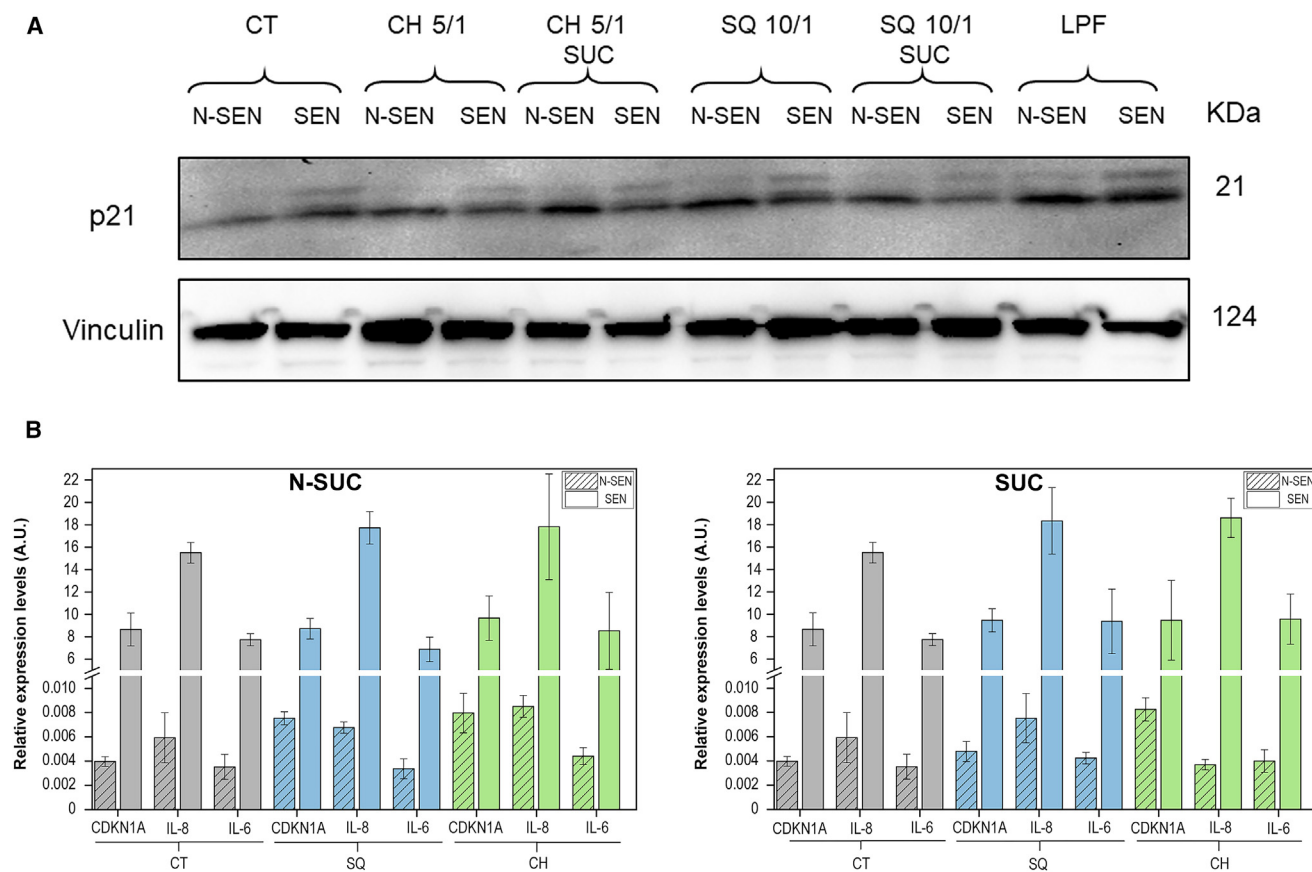
Figure 8. Relative expression levels of senescence markers

Western blot representative image of p21 and vinculin expression levels (A) and senescence markers associated with cell-cycle arrest (CDKN1A) and SASP (IL-8 and IL-6) normalized with the expression levels of the housekeeping gene ACTB (B), measured at 72 h post-transfection of non-senescent (N-SEN) and senescent (SEN) cells un-transfected (control; CT) or transfected using niosome formulations of squalene (SQ) or cholesterol (CH) prepared in the absence (N-SUC) or presence (SUC) of sucrose at DOTMA/DNA ratios of 10/1 and 5/1, respectively. Data are shown as mean ± SD.

lower panels), suggesting that the entry of nioplexes into senescent cells takes place by macropinocytosis.

Finally, to study if transfection using niosomes could affect the senescence profile of UC-MSCs, we evaluated main senescence markers after cell transfection with SQ or CH niosomes at DOTMA/DNA ratios of 5/1 and 10/1. Similar to that observed in untransfected cells (Figure S3B), a statistically significant reduction of cell density was demonstrated in UC-MSC senescent cells compared with non-senescent cells (p < 0.01) (Figure S3B). Alongside, an increase in p21 expression was demonstrated in transfected senescent cells when compared with those levels observed in transfected non-senescent cells (Figures 8A and S8). Therefore, the levels of mRNA expression of senescence markers associated with cell-cycle arrest (*CDKN1A*) and SASP (*IL-8* and *IL-6*) were significantly higher in senescent UC-MSCs when compared with non-senescent UC-MSCs transfected with the two formulations in the absence and presence of SUC (p ≤ 0.01) (Figure 8B).

DISCUSSION

MSCs are a pivotal population in regenerative medicine for the treatment of several pathologies including those associated with the nervous system, musculoskeletal system, myocardium, liver, cornea, trachea, and skin.[48] However, the properties of this outstanding cell population are weakened with aging resulting in a decrease in its number, which may impair tissue homeostasis, regeneration, and repair. Therefore, the development of anti-aging therapies to preserve native properties of MSCs or even revert their senescent phenotype, has gained special relevance in the last decades. Senodrugs (senolytics and senomorphics) constitute the first-line therapeutic agents to target senescent cells.[49,50] Despite these drugs having been extensively studied to decrease the accumulation of senescent cells in tissues or organs, their use is still limited by their potential side effects.[51]

Therefore, the search for alternative therapies to target senescent cells is under investigation. Some approaches include the design of galacto-oligosaccharide-coated nanoparticles containing cytotoxic

(doxorubicin) or senolytic (navitoclax) drugs that are released upon degradation by lysosomal SA-β-galactosidase.[52] Other strategies include nanoparticles functionalized with antibodies against CD9 cell membrane receptor,[53] core-shell spiky nanorods coated with antibodies against the aB2MG coat,[54] or chiral CuxCoyS nanoparticles for selective targeting of senescent cells.[55] A last approach includes the use of pro-drugs that selectively kill senescent cells such as Nav-Gal being activated through cleavage of (acetylated) galactose modification by lysosomal SA-β-galactosidase of senescent cells[56] and proteolysis-targeting chimera to reduce the toxicity of senolytics.[57]

Still, and despite the significant progress made in this field, the use of these therapies is still limited by the heterogeneity of senescence biomarkers on the surfaceome, secretome, and metabolome, and intracellular signaling of senescent cells[58] and the excessive elimination of aging-associated senescent cells in some tissues.[59]

Therefore, gene editing and gene delivery have emerged as attractive alternative therapies to modify cell fate in aging with low toxicity and high efficiency in comparison with senodrugs.[60,61] In this scenario numerous studies have tested the possibility to genetically modify senescent cells such as chondrocytes,[62] pancreatic cells,[63] or hematopoietic and vascular cells[64] as main targets in age-related diseases such as osteoarthritis,[62] diabetes,[63] pulmonary fibrosis,[65] cardiovascular diseases,[64] or autoimmune diseases.[66,67]

Gene therapy applied to MSCs constitutes a promising tool to increase their therapeutic potential for the treatment of several pathologies including those related with aging.[21–23] However, MSCs are complex cell populations exhibiting a high heterogeneity that comprises proliferation rate, morphology, immunophenotype, multilineage differentiation potential, and senescence. All these factors hamper genetic modification of senescent MSCs using classical viral and non-viral liposomal-like systems.[68]

Niosomes have arisen as potential non-viral nanocarriers with tunable properties to genetically modify MSCs in various regenerative medicine approaches.[24,29,31] However, none of these studies have tested the possibility of using niosomes to genetically modify MSCs with a senescent phenotype.

Based on this, in the present study we examined, for the first time to the best of our knowledge, the possibility of using non-viral systems based on niosomes for the genetic modification of senescent MSCs.

The data from the study first revealed an influence on helper lipid composition on physicochemical features of niosomes and nioplexes. Therefore, niosomes formulated with CH were significantly bigger than those formulated with SQ, with a marked higher electropositivity. Of note, the addition of sucrose to CH niosome formulations reduced their polydispersity, as noted by their lower PDI values.

The size of the nioplexes is essential to ensure that they interact properly with the different cellular components. In this sense, it has been observed that a reduced size of the nioplexes constitutes an advantage to the cellular internalization.[69,70] In concordance with previous studies,[34] the size of CH nioplexes formulated without sucrose showed discrete oscillations in particle size upon addition of pEGFP. These observations may be attributed to the balance between larger space demanded by the cationic lipid and the greater DNA condensation when increasing mass ratio,[24] as confirmed by the gradual increment on DNA complexation observed in CH nioplexes. In contrast, the sizes of SQ-based nioplexes were more stable as noted by the plateau observed in DNA complexation studies. Addition of sucrose to niosome formulations led to an increment in size of SQ nioplexes without differences in their complexation ability. Conversely, no substantial differences were observed in CH nioplexes formulated with sucrose, despite the addition of this sugar leading to lower PDI values and higher complexation ability.

It is known that the presence of a positive surface in nioplexes promotes their entry into cells due to their electrostatic interaction with the negative charges of the glycocalyx in the first steps of endocytosis.[29] In this context, the highest values of electropositivity were reached at DOTMA/DNA ratios of 10/1 in SQ nioplexes and at 5/1 and 15/1 in CH complexes. Finally, agarose gel electrophoresis assays showed that both niosome formulations were able to condense, release, and protect DNA against DNase I enzymatic digestion, as confirmed by the presence of SC bands.[24]

To test the performance of the developed formulations for gene delivery purposes in senescent cells we stablished a model of senescence in UC-MSCs isolated using a TIS model with the selective inhibitor of CDK4/6, Palbociclib.[47] In good concordance with their superior values of electropositivity, the highest levels of GFP transgene expression in non-senescent UC-MSCs were achieved with SQ niosome formulations at a cationic lipid/DNA ratio of 10/1. These results are in good agreement with previous studies using niosomes based in DOTMA, SQ, and P20 to transfect primary retina cells.[34,35] Conversely, and in concordance with their higher values of electropositivity, the highest levels of transgene expression in senescent cells were achieved with CH nioplexes at a DOTMA/DNA ratio of 5/1. These findings highlight the need to achieve an adequate balance between complex stability and their ability to deliver the DNA molecules inside the cell to achieve an effective transfection.[43] As a matter of fact, previous studies have suggested that high cholesterol levels are possibly a feature of cell senescence, cholesterol accumulation being a driver of senescence.[71] However, this fact may in part be the reason for the higher levels of transgene expression obtained with CH nioplexes; additional studies will be necessary to explain this observation.

Furthermore, the addition of sucrose into the niosome formulations increased the levels of GFP expression, mostly when using SQ nioplexes independently of the cell phenotype, although this was more prominent in senescent cells.

Of note, and in marked contrast to that observed with LPF, transfection of UC-MSCs via niosome formulations led always to high levels of cell viability, being in the range of 94%–99% in non-senescent cells

and from 92% to 99% in senescent cells. These results are in agreement with previous results showing a reduction of MSC viability in the presence of the lipoplexes.[24]

Since transfection efficiency is highly conditioned by endocytosis, being dependent on the cell type,[72] we performed transfection studies in the presence of known endocytosis inhibitors to determine the preferential uptake mechanism of nioplexes in senescent and non-senescent cells. To this end, we established the best conditions relative to cell inhibitor concentrations and incubation times able to retain cell viability values greater than 86%.

Our findings showed that internalization of nioplexes in non-senescent cells predominantly takes places by caveolae-mediated endocytosis. These results are in good agreement with those of Vanegas Saenz et al. showing a preferential uptake of octa-arginine functionalized calcium phosphate nanoparticles in MSCs by this route.[73]

Conversely, in senescent UC-MSCs, nioplexes were internalized by macropinocytosis. Macropinocytosis is a clathrin- and dynamin-independent endocytic process through large irregular vacuoles called macropinosomes, which are essential for the endosomal escape of the DNA associated with non-viral vectors.[74,75] The preferential internalization of nioplexes by this route in senescent cells may be attributed to the prevalence of a lymphocyte antigen 6 complex-induced macropinocytosis as a cell survival mechanism of senescent cells.[74] Our data are in accordance with Shin et al.[76] and Wheaton et al.[77] They have shown that senescent cells have a loss of functional clathrin- and caveolin-dependent endocytosis and activated macropinocytosis.

Therefore, we can confirm that the non-viral systems developed in the present study constitute suitable tools for genetic modification of senescent MSCs. Taken together, we provide a potential strategy to rejuvenate or eliminate senescent cells to treat age-related diseases. Future studies will involve the complexation of niosome formulations with other conventional plasmids or DNA minicircles for therapeutic targeting of senescent MSCs.

MATERIALS AND METHODS

Cell culture

Human UCs were obtained from caesarean sections performed on healthy women at the Maternity Facility at Complejo Hospitalario Universitario A Coruña (CHUAC). All tissues were obtained with fully informed consent and ethical approval by the supervisor of the Ethical Committee (CEIC: 2019/026) of Galicia. All the women were between 26 and 35 years. MSCs were isolated from UCs using the protocol developed by Arufe and colleagues' biobank.[47] In brief, the tissue was washed with PBS, placed in 100-mm culture dishes, cut into small pieces (explants), incubated for three 5-min periods in an enzyme mixture containing 1.2 U/mL dispase and 11.2 U/mL type I collagenase (all from Sigma-Aldrich, Madrid, Spain) and cultured in Dulbeccós modified Eagle's medium with 10% (v/v) fetal bovine serum, 1% (v/v) penicillin, and 1% (v/v) streptomycin (all

from Sigma-Aldrich) (growth medium). UC-MSCs were allowed to attach to the plastic dishes for 3 days before removing the explants and maintaining them in growth medium at 37°C in a humidified atmosphere containing 5% CO_2. T/C-28a2 immortalized healthy chondrocytes from human costal cartilage from a 15-year-old female (SCC042) (Sigma-Aldrich) (TC28a2) were grown in growth medium and kept at 37°C in a humidified atmosphere containing 5% CO_2.

Characterization of UC-MSCs by FACS

UC-MSCs were washed twice in PBS and incubated with the appropriate concentrations of primary antibodies (Table S2) for 1 h at room temperature. Negative control staining was performed using the isotype (Table S2). After incubation, cells were washed twice with PBS and analyzed using a cytometer FACSAria (BD Science, Madrid, Spain). A TC28a2 healthy chondrocytes cell line was used as negative control of expression of undifferentiation markers. Data were generated by BD FACSDiva software (BD Science, San Jose, CA).

Induction of senescence in UC-MSCs

Cells (passage 4) were seeded in 48-well plates (15,000 cells/well) and allowed to attach for 24 h before performing the experiments. Cellular senescence was induced in proliferative UC-MSCs using TIS.[47] UC-MSCs were cultured in growth medium and treated (senescent cells) or not (non-senescent cells) with 1 μM Palbociclib (CDK4/6 inhibitor) (MedChemexpress, NJ) for 6 days (Figure S3A). After this time, cells were washed with PBS and cultured in growth medium for an additional 2 days before different studies. Half of the plates were used for the analysis of senescence phenotype (proliferation and gene expression profiles) and the other half for transfection assays (GFP transgene expression, apoptosis, and gene expression profiles).

Analysis of UC-MSC proliferation

Plates were fixed using 4% (v/v) paraformaldehyde for 15 min at room temperature and washed three times with PBS. Then, the plates were stained with 0.5% (v/v) crystal violet solution and scanned. The quantification of crystal violet was performed by solubilizing crystal violet staining (Sigma-Aldrich) with 30% (v/v) acetic acid and measuring the absorbance at 570 nm using a NanoQuant microplate reader (Tecan Trading, Switzerland).

Assessment of UC-MSC senescence phenotype

Total RNA from cells was extracted using TRIzol Reagent (Thermo Fisher Scientific, Foster City, CA) according to the manufacturer's instructions. cDNA synthesis was performed using a high-capacity cDNA reverse transcriptase kit (Thermo Fisher Scientific). qPCR reactions were performed using SYBR Green PCR Master Mix (Applied Biosystems, Foster City, CA) and primers for CDKN1A, IL-8, and IL-6 markers (Table S3) using LightCycler 480 (Roche, Basel, Switzerland).

Immunoblot

The proteins from cells were isolated using the RIPA lysis buffer (150 mM sodium chloride, 50 mM Tris-base, 0.1% [p/v] sodium dodecyl sulfate, Triton 1% [v/v] [all from Sigma-Aldrich, San Diego,

CA]). Lysates were diluted in 4× Laemmli buffer (Bio-Rad, CA) obtaining the same concentration of proteins (20 μg) for each sample. The proteins were separated in SDS-PAGE gels and transferred into PVDF membrane with 0.45-mm pore size (Millipore, MA, USA). This membrane was incubated for 1 h with the blocking buffer (5% [w/v] bovine serum albumin) (Sigma-Aldrich). Then we added the primary antibody at suitable concentration (Table S2), which was incubated overnight at 4°C. The following day the membrane was washed at least three times 10 min before adding the secondary antibody (Table S2), which was incubated overnight again. Another three washes were made before revealing the protein expression with the ECL substrate (Millipore, MA) using a ChemiDocMP Imaging System (Bio-Rad).

Niosome preparation

Niosomes were prepared using a reversed-phase evaporation technique.[78] In brief, P20 (15 mg), PX (15 mg), DOTMA (2 mg), and SQ (5 mg) or CH (5 mg) were dissolved together in dichloromethane (1 mL) and emulsified with 3 mL of OptiMEM medium. The mixture was sonified for 30 s at 45% amplitude using a UP200S Sonifier (Hielscher Ultrasound Technology, Germany) with a 1-mm probe. The organic solvent was then removed by evaporation at room temperature under magnetic stirring for 3 h, obtaining the dispersion of niosomes in the aqueous medium. Resulting niosome formulations were denoted as CH (niosomes composed of DOTMA, P20, PX, and cholesterol) or SQ (niosomes composed of DOTMA, P20, PX, and SQ), respectively.

Niosome dispersions with sucrose were prepared by the same method but using OptiMEM with 300 mM sucrose as aqueous medium.

Plasmid propagation and formation of nioplexes

The p0DB-001_pEGFP-N1 (pEGFP) was kindly donated by Dr. Romero-Saavedra (University of Munich) and propagated, purified, and quantified following standard procedures. Nioplexes were generated by mixing a fixed volume of the plasmid stock solution (700 ng) with increasing volumes of each niosome formulation. Cationic lipids for a fixed amount of DNA mass ratios (w/w) of nioplexes were 5/1, 10/1, 15/1, and 20/1, equivalent to cationic amino groups (N) to nucleic acid anionic phosphate groups (P) ratios of 2, 5, 7, and 10, respectively.[24] The mixtures were incubated at room temperature for 30 min to promote the electrostatic interactions between the niosomes and the negative charge of the plasmid.[24,30]

Physicochemical characterization of niosomes and nioplexes
Size and Z potential

CH and SQ niosomes and their nioplexes (cationic lipid/DNA mass ratios of 5/1, 10/1, 15/1, and 20/1) were prepared following the same procedure described in the previous section. The size and Z potential (triplicate) of both niosomes and nioplexes were assessed at 20°C by dynamic light scattering and electrophoretic light scattering using a NanoBrook 90Plus Zeta (Brookhaven Instruments, Holtsville, NY). In brief, niosome formulations were diluted (1:10) in water and particle size was obtained by cumulative analysis. The Smoluchowski

approximation was used to support the calculation of the Z potential from the electrophoretic mobility. Measurements were performed using folded capillary cuvettes (DTS1070).

Agarose gel electrophoresis

The capacity of both SQ and CH niosome formulations to protect the DNA was evaluated by agarose gel electrophoresis assay of nioplexes formed at cationic lipid/DNA mass ratios (w/w) of 5/1, 10/1, 15/1, and 20/1. The mixtures were incubated at 37°C for 30 min after adding DNase I (0.4 U/μg DNA).[29] Finally, 7% SDS solution (3 μL) was added to release DNA from the nioplexes, and the samples were run on a 0.8% w/v agarose gel, immersed in TBE buffer, and exposed for 45 min to 90 V. DNA bands were stained with SYBR Gold, and images were observed under a digital Chemi-Doc MP Imaging System (Bio-Rad, Madrid, Spain). Naked GFP was used as negative control (cationic lipid/DNA [w/w] mass ratio of 0).

Evaluation of niosome complexation ability

The ability of SQ and CH niosomes to complex DNA was evaluated by means of a fluorescence-exclusion titration assay.[79] In brief, SQ and CH nioplexes were prepared, as described previously, by mixing 0.5 μg of DNA with the corresponding amount of niosomes. The samples were incubated, protected from light, with SYBR Gold (200×; 3 μL) for 10 min and, finally, 10 mM HEPES was added to reach a final volume of 100 μL/well. Fluorescence measurements were performed with a Synergy HTX Plate Reader (Biotek, Winooski, VT) in 96-black-well plates (λ_{exc} = 485nm, λ_{em} = 528 nm). The DNA complexation efficiency (%) was expressed as relative fluorescence, normalized to the fluorescence of uncomplexed (naked) DNA according to the following equation:

$$\text{Relative fluorescence } (\%) \ = \ \frac{F_{\text{sample}} \ - \ F_{\text{blank}}}{F_{\text{naked pDNA}} \ - \ F_{\text{blank}}} \times 100$$

In this equation F_{sample} depicts the fluorescence intensity of each sample and F_{blank} represents the fluorescence values recorded from the blank, performed by using the same dilution of SYBR Green (200×) in 10 mM HEPES. Each condition was assessed in triplicate.

Transmission electron microscopy

Drops of SQ or CH niosome dispersions (5 μL) were placed on carbon-coated grids. The excess was carefully removed with a filter paper. Samples were dyed with 2% (v/v) uranyl acetate (Sigma-Aldrich), dried, and observed using a high-resolution JEM-1011 TEM (JEOL USA, Peabody, MA).[24]

Transfection assays

Prior to transfection assays, UC-MSCs were cultured in 48-well plates for 6 days in the absence (non-senescent cells UC-MSCs) or presence (senescent cells UC-MSCs) of 1 μM Palbociclib, as described before (see section induction of senescence in UC-MSCs). Non-senescent and senescent cells were exposed to different nioplexes formed upon complexation of SQ or CH niosome formulations with pEGFP (always 700 ng of plasmid) at DOTMA/DNA (w/w) ratios

of 5/1, 10/1, 15/1, and 20/1. UC-MSCs cultured in OptiMEM medium without nioplexes or transfected with LPF (3.5 μL/well) were used as negative and positive controls, respectively. Cells were incubated with nioplexes or LPF lipoplexes for 3 h at 37°C and 5% CO_2. Afterward, medium was removed and replenished with growth medium, and cells were cultured for 24 and 72 h until analyses.

Transfection efficiency

The transfection efficiency achieved with nioplexes was evaluated using fluorescence-activated cell sorting (FACS). In brief, cells were collected in FACS tubes, washed three times with PBS, and the fluorescence of fluorescein isothiocyanate analyzed using a cytometer FACSAria (BD Science, Madrid, Spain). The FACS data were generated by BD FACSDiva software (BD Science, San Jose, CA). Parallel, GFP fluorescence was monitored using a fluorescence microscope (Nikon Eclipse TI, Nikon, Tokyo, Japan).

Cellular uptake of nioplexes

Cells were cultured in 48-well plates for 6 days in the absence of 1 μM Palbociclib, as described in induction of senescence in UC-MSCs and pre-treated with the following inhibitors at an optimized dose overtime[80,81]: chlorpromazine as clathrin-mediated endocytosis inhibitor (30 μM, 1 h), genistein as caveolae-mediated endocytosis inhibitor (200 μM, 1 h), methyl-β-cyclodextrin as clathrin- and caveolae-dependent endocytosis inhibitor (2 mM, 10 min); and amiloride as macropinocytosis inhibitor (5 mM, 10 min). After pre-treatment, CH or SQ nioplexes at DOTMA/DNA ratios of 5/1 and 10/1, respectively, were added and incubated for 4 h. Control conditions included cells transfected with nioplexes without inhibitor treatment. Transfection efficiency achieved with nioplexes was assessed by AR1 confocal microscopy (Nikon) and FACS, as described in transfection efficiency.

Cell viability

Cell viability upon contact with nioplexes was evaluated by crystal violet staining using the same protocol described in analysis of UC-MSC proliferation. Apoptosis was also assessed using the Annexin V Alexa Fluor 647 conjugate (Immunostep, Salamanca, Spain). In brief, cells were collected in FACS tubes (Thermo Fisher Scientific, Madrid, Spain) and incubated with Annexin V-647 (25 μg/mL) for 10 min in darkness at room temperature. Propidium iodide staining solution (1 μg/mL) was then added and cell fluorescence analyzed using a FACSAria. The FACS data were generated by BD FACSDiva software (BD Science, San Jose, CA).

Analysis of senescence markers after transfection

Expression of *CDKN1A*, *IL-8*, and *IL-6* (Table S3) in senescent and non-senescent UC-MSCs were evaluated 24 and 72 h after transfection by qPCR using the same procedures described in assessment of UC-MSC senescence phenotype.

Statistical analysis

Studies were performed in UC-MSCs isolated from six patients and measurements were performed in triplicate. Data are expressed as mean ± standard deviation (SD). The graphs were generated using OriginPro 8.5.1. Statistical analyses were performed using R x64 3.5.1., RStudio by parametric tests (two- and three-way ANOVA; Tukey's test; Student's t-test) and non-parametric ones (Kruskal-Wallis). $p < 0.05$ was considered statistically significant.

DATA AND CODE AVAILABILITY

All data reported in this paper will be shared by the lead contacts upon request.

SUPPLEMENTAL INFORMATION

Supplemental information can be found online at https://doi.org/10.1016/j.omtn.2023.03.010.

AUTHOR CONTRIBUTIONS

Conceptualization, J.F.-L. and A.R.-R.; methodology, J.F.-L., A.R.-R., J.L.-S., D.M.-B., and N.C.-P.; writing – original draft, J.F.-L., A.R.-R., J.L.-S., D.M.-B., and A.I.-F.; writing – review & editing, J.F.-L. A.R.-R., and M.C.-A.; experimental assays, J.L.-S., D.M.-B., N.C.-P., A.I.-F., and M.S.-S. All authors read and approved the final manuscript.

DECLARATION OF INTERESTS

The authors declare no competing interests.

REFERENCES

1. Fafián-Labora, J.A., and O'Loghlen, A. (2020). Classical and nonclassical intercellular communication in senescence and ageing. Trends Cell Biol. *30*, 628–639.

2. Raisz, L.G. (1988). Local and systemic factors in the pathogenesis of osteoporosis. N. Engl. J. Med. *318*, 92–101.

3. Querfurth, H.W., and LaFerla, F.M. (2010). Alzheimer's disease. N. Engl. J. Med. *362*, 329–344.

4. Kwon, Y.H., Fingert, J.H., Kuehn, M.H., and Alward, W.L.M. (2009). Primary open-angle glaucoma. N. Engl. J. Med. *360*, 1113–1124.

5. de Magalhães, J.P. (2013). How ageing processes influence cancer. Nat. Rev. Cancer *13*, 357–365.

6. Gunasekaran, U., and Gannon, M. (2011). Type 2 diabetes and the aging pancreatic beta cell. Aging (Albany NY) *3*, 565–575.

7. McHugh, D., and Gil, J. (2018). Senescence and aging: causes, consequences, and therapeutic avenues. J. Cell Biol. *217*, 65–77.

8. Xiang, X.N., Zhu, S.Y., He, H.C., Yu, X., Xu, Y., and He, C.Q. (2022). Mesenchymal stromal cell-based therapy for cartilage regeneration in knee osteoarthritis. Stem Cell Res. Ther. *13*, 14.

9. Venkatesh, K., and Sen, D. (2017). Mesenchymal stem cells as a source of dopaminergic neurons: a potential cell based therapy for Parkinson's disease. Curr. Stem Cell Res. Ther. *12*, 326–347.

10. Zarbin, M. (2019). Cell-based therapy for retinal disease: the new frontier. Methods Mol. Biol. *1834*, 367–381.

11. Fafián-Labora, J.A., Morente-López, M., and Arufe, M.C. (2019). Effect of aging on behaviour of mesenchymal stem cells. World J. Stem Cell. *11*, 337–346.

12. Miceli, V., Bulati, M., Iannolo, G., Zito, G., Gallo, A., and Conaldi, P.G. (2021). Therapeutic properties of mesenchymal stromal/stem cells: the need of cell priming for cell-free therapies in regenerative medicine. Int. J. Mol. Sci. *22*, 763–820.

13. Kleiman, R.J., and Engle, S.J. (2021). Human inducible pluripotent stem cells: realization of initial promise in drug discovery. Cell Stem Cell *28*, 1507–1515.

14. de Koning, E.J.P., and Carlotti, F. (2021). Stem cell-based islet replacement therapy in diabetes: a road trip that reached the clinic. Cell Stem Cell *28*, 2044–2046.

15. Janzen, V., Forkert, R., Fleming, H.E., Saito, Y., Waring, M.T., Dombkowski, D.M., Cheng, T., DePinho, R.A., Sharpless, N.E., and Scadden, D.T. (2006). Stem-cell ageing modified by the cyclin-dependent kinase inhibitor p16INK4a. Nature *443*, 421–426.

16. Yang, Y.M., Li, P., Cui, D.C., Dang, R.J., Zhang, L., Wen, N., and Jiang, X.X. (2015). Effect of aged bone marrow microenvironment on mesenchymal stem cell migration. Age *37*, 16.

17. Chen, D., and Kerr, C. (2019). The epigenetics of stem cell aging comes of age. Trends Cell Biol. *29*, 563–568.

18. Ou, H.L., Hoffmann, R., González-López, C., Doherty, G.J., Korkola, J.E., and Muñoz-Espín, D. (2021). Cellular senescence in cancer: from mechanisms to detection. Mol. Oncol. *15*, 2634–2671.

19. Wang, L., Lankhorst, L., and Bernards, R. (2022). Exploiting senescence for the treatment of cancer. Nat. Rev. Cancer *22*, 340–355.

20. Moskalev, A., Guvatova, Z., Lopes, I.D.A., Beckett, C.W., Kennedy, B.K., De Magalhaes, J.P., and Makarov, A.A. (2022). Targeting aging mechanisms: pharmacological perspectives. Trends Endocrinol. Metab. *33*, 266–280.

21. Madry, H., and Cucchiarini, M. (2016). Gene therapy for human osteoarthritis: principles and clinical translation. Expet Opin. Biol. Ther. *16*, 331–346.

22. Wang, X., Wang, H., Lu, J., Feng, Z., Liu, Z., Song, H., Wang, H., Zhou, Y., and Xu, J. (2020). Erythropoietin-Modified mesenchymal stem cells enhance anti-fibrosis efficacy in mouse liver fibrosis model. Tissue Eng. Regen. Med. *17*, 683–693.

23. Xue, B., Xiao, X., Yu, T., Xiao, X., Xie, J., Ji, Q., Wang, L., Na, T., Meng, S., Qian, L., and Duan, H. (2021). Mesenchymal stem cells modified by FGF21 and GLP1 ameliorate lipid metabolism while reducing blood glucose in type 2 diabetic mice. Stem Cell Res. Ther. *12*, 133.

24. Carballo-Pedrares, N., Kattar, A., Concheiro, A., Alvarez-Lorenzo, C., and Rey-Rico, A. (2021). Niosomes-based gene delivery systems for effective transfection of human mesenchymal stem cells. Mater. Sci. Eng. C Mater. Biol. Appl. *128*, 112307.

25. Yin, H., Kanasty, R.L., Eltoukhy, A.A., Vegas, A.J., Dorkin, J.R., and Anderson, D.G. (2014). Non-viral vectors for gene-based therapy. Nat. Rev. Genet. *15*, 541–555.

26. Mitchell, M.J., Billingsley, M.M., Haley, R.M., Wechsler, M.E., Peppas, N.A., and Langer, R. (2021). Engineering precision nanoparticles for drug delivery. Nat. Rev. Drug Discov. *20*, 101–124.

27. Puras, G., Martínez-Navarrete, G., Mashal, M., Zárate, J., Agirre, M., Ojeda, E., Grijalvo, S., Eritja, R., Diaz-Tahoces, A., Avilés-Trigueros, M., et al. (2015). Protamine/DNA/Niosome ternary nonviral vectors for gene delivery to the retina: the role of protamine. Mol. Pharm. *12*, 3658–3671.

28. Ojeda, E., Puras, G., Agirre, M., Zarate, J., Grijalvo, S., Eritja, R., Martinez-Navarrete, G., Soto-Sánchez, C., Diaz-Tahoces, A., Aviles-Trigueros, M., et al. (2016). The influence of the polar head-group of synthetic cationic lipids on the transfection efficiency mediated by niosomes in rat retina and brain. Biomaterials *77*, 267–279.

29. Attia, N., Mashal, M., Grijalvo, S., Eritja, R., Zárate, J., Puras, G., and Pedraz, J.L. (2018). Stem cell-based gene delivery mediated by cationic niosomes for bone regeneration. Nanomedicine *14*, 521–531.

30. Attia, N., Mashal, M., Puras, G., and Pedraz, J.L. (2021). Mesenchymal stem cells as a gene delivery tool: promise, problems, and prospects. Pharmaceutics *13*, 843.

31. Villate-Beitia, I., Truong, N.F., Gallego, I., Zárate, J., Puras, G., Pedraz, J.L., and Segura, T. (2018). Hyaluronic acid hydrogel scaffolds loaded with cationic niosomes for efficient non-viral gene delivery. RSC Adv. *8*, 31934–31942.

32. Gallego, I., Villate-Beitia, I., Martínez-Navarrete, G., Menéndez, M., López-Méndez, T., Soto-Sánchez, C., Zárate, J., Puras, G., Fernández, E., and Pedraz, J.L. (2019). Non-viral vectors based on cationic niosomes and minicircle DNA technology enhance gene delivery efficiency for biomedical applications in retinal disorders. Nanomedicine *17*, 308–318.

33. Gallego, I., Villate-Beitia, I., Soto-Sánchez, C., Menéndez, M., Grijalvo, S., Eritja, R., Martínez-Navarrete, G., Humphreys, L., López-Méndez, T., Puras, G., et al. (2020). Brain angiogenesis induced by nonviral gene therapy with potential therapeutic benefits for central nervous system diseases. Mol. Pharm. *17*, 1848–1858.

34. Villate-Beitia, I., Gallego, I., Martínez-Navarrete, G., Zárate, J., López-Méndez, T., Soto-Sánchez, C., Santos-Vizcaíno, E., Puras, G., Fernández, E., and Pedraz, J.L. (2018). Polysorbate 20 non-ionic surfactant enhances retinal gene delivery efficiency of cationic niosomes after intravitreal and subretinal administration. Int. J. Pharm. *550*, 388–397.

35. Gallego, I., Villate-Beitia, I., Martínez-Navarrete, G., Menéndez, M., López-Méndez, T., Soto-Sánchez, C., Zárate, J., Puras, G., Fernández, E., and Pedraz, J.L. (2019). Non-viral vectors based on cationic niosomes and minicircle DNA technology enhance gene delivery efficiency for biomedical applications in retinal disorders. Nanomedicine *17*, 308–318.

36. Mashal, M., Attia, N., Soto-Sánchez, C., Martínez-Navarrete, G., Fernández, E., Puras, G., and Pedraz, J.L. (2018). Non-viral vectors based on cationic niosomes as efficient gene delivery vehicles to central nervous system cells into the brain. Int. J. Pharm. *552*, 48–55.

37. Gallego, I., Villate-Beitia, I., Soto-Sánchez, C., Menéndez, M., Grijalvo, S., Eritja, R., Martínez-Navarrete, G., Humphreys, L., López-Méndez, T., Puras, G., et al. (2020). Brain angiogenesis induced by nonviral gene therapy with potential therapeutic benefits for central nervous system diseases. Mol. Pharm. *17*, 1848–1858.

38. Grijalvo, S., Alagia, A., Puras, G., Zárate, J., Mayr, J., Pedraz, J.L., Eritja, R., and Díaz, D.D. (2017). Cationic nioplexes-in-polysaccharide-based hydrogels as versatile biodegradable hybrid materials to deliver nucleic acids. J. Mater. Chem. B *5*, 7756–7767.

39. Al Qtaish, N., Gallego, I., Villate-Beitia, I., Sainz-Ramos, M., López-Méndez, T.B., Grijalvo, S., Eritja, R., Soto-Sánchez, C., Martínez-Navarrete, G., Fernández, E., et al. (2020). Niosome-based approach for in situ gene delivery to retina and brain cortex as immune-privileged tissues. Pharmaceutics *12*, 198.

40. Puras, G., Mashal, M., Zárate, J., Agirre, M., Ojeda, E., Grijalvo, S., Eritja, R., Diaz-Tahoces, A., Martínez Navarrete, G., Avilés-Trigueros, M., et al. (2014). A novel cationic niosome formulation for gene delivery to the retina. J. Contr. Release *174*, 27–36.

41. Ojeda, E., Puras, G., Agirre, M., Zárate, J., Grijalvo, S., Pons, R., Eritja, R., Martinez-Navarrete, G., Soto-Sanchez, C., Fernández, E., and Pedraz, J.L. (2015). Niosomes based on synthetic cationic lipids for gene delivery: the influence of polar head-groups on the transfection efficiency in HEK-293, ARPE-19 and MSC-D1 cells. Org. Biomol. Chem. *13*, 1068–1081.

42. Qin, Y., Tian, Y., Liu, Y., Li, D., Zhang, H., Yang, Y., Qi, J., Wang, H., and Gan, L. (2018). Hyaluronic acid-modified cationic niosomes for ocular gene delivery: improving transfection efficiency in retinal pigment epithelium. J. Pharm. Pharmacol. *70*, 1139–1151.

43. Carballo-Pedrares, N., Sanjurjo-Rodriguez, C., Señarís, J., Díaz-Prado, S., and Rey-Rico, A. (2022). Chondrogenic differentiation of human mesenchymal stem cells via SOX9 delivery in cationic niosomes. Pharmaceutics *14*, 2327.

44. Ojeda, E., Puras, G., Agirre, M., Zarate, J., Grijalvo, S., Eritja, R., Digiacomo, L., Caracciolo, G., and Pedraz, J.L. (2016). The role of helper lipids in the intracellular disposition and transfection efficiency of niosome formulations for gene delivery to retinal pigment epithelial cells. Int. J. Pharm. *503*, 115–126.

45. Lidzbarsky, G., Gutman, D., Shekhidem, H.A., Sharvit, L., and Atzmon, G. (2018). Genomic instabilities, cellular senescence, and aging: in vitro, in vivo and aging-like human syndromes. Front. Med. *5*, 104.

46. Hsu, H.-C., Chen, J., and Mountz, J.D. (2019). Gene therapy and immunosenescence. Handb. Immunosenescence, 2795–2820.

47. Mato-Basalo, R., Morente-López, M., Arntz, O.J., van de Loo, F.A.J., Fafián-Labora, J., and Arufe, M.C. (2021). Therapeutic potential for regulation of the nuclear factor kappa-B transcription factor p65 to prevent cellular senescence and activation of pro-inflammatory in mesenchymal stem cells. Int. J. Mol. Sci. 22, 3367.

48. Han, Y., Li, X., Zhang, Y., Han, Y., Chang, F., and Ding, J. (2019). Mesenchymal stem cells for regenerative medicine. Cells 8, 886.

49. Li, C., Chai, Y., Wang, L., Gao, B., Chen, H., Gao, P., Zhou, F.Q., Luo, X., Crane, J.L., Yu, B., et al. (2017). Programmed cell senescence in skeleton during late puberty. Nat. Commun. 8, 1312.

50. Hall, B.M., Balan, V., Gleiberman, A.S., Strom, E., Krasnov, P., Virtuoso, L.P., Rydkina, E., Vujcic, S., Balan, K., Gitlin, I.I., et al. (2017). p16(Ink4a) and senescence-associated β-galactosidase can be induced in macrophages as part of a reversible response to physiological stimuli. Aging (Albany NY) 9, 1867–1884.

51. Kirkland, J.L., Tchkonia, T., Zhu, Y., Niedernhofer, L.J., and Robbins, P.D. (2017). The clinical potential of senolytic drugs. J. Am. Geriatr. Soc. 65, 2297–2301.

52. González-Gualda, E., Pàez-Ribes, M., Lozano-Torres, B., Macias, D., Wilson, J.R., González-López, C., Ou, H.L., Mirón-Barroso, S., Zhang, Z., Lérida-Viso, A., et al. (2020). Galacto-conjugation of Navitoclax as an efficient strategy to increase senolytic specificity and reduce platelet toxicity. Aging Cell 19, e13142.

53. Thapa, R.K., Nguyen, H.T., Jeong, J.H., Kim, J.R., Choi, H.G., Yong, C.S., and Kim, J.O. (2017). Progressive slowdown/prevention of cellular senescence by CD9-targeted delivery of rapamycin using lactose-wrapped calcium carbonate nanoparticles. Sci. Rep. 7, 43299.

54. Lu, M., Qu, A., Li, S., Sun, M., Xu, L., Kuang, H., and Xu, C. (2020). Mitochondria-targeting plasmonic spiky nanorods increase the elimination of aging cells in vivo. Angew Chem. Int. Ed. Engl. 59, 8698–8705.

55. Li, S., Sun, M., Hao, C., Qu, A., Wu, X., Xu, L., Xu, C., and Kuang, H. (2020). Chiral Cu x Co y S nanoparticles under magnetic field and NIR light to eliminate senescent cells. Angew Chem. Int. Ed. Engl. 59, 13915–13922.

56. Cai, Y., Zhou, H., Zhu, Y., Sun, Q., Ji, Y., Xue, A., Wang, Y., Chen, W., Yu, X., Wang, L., et al. (2020). Elimination of senescent cells by β-galactosidase-targeted prodrug attenuates inflammation and restores physical function in aged mice. Cell Res. 30, 574–589.

57. He, Y., Zhang, X., Chang, J., Kim, H.N., Zhang, P., Wang, Y., Khan, S., Liu, X., Zhang, X., Lv, D., et al. (2020). Using proteolysis-targeting chimera technology to reduce navitoclax platelet toxicity and improve its senolytic activity. Nat. Commun. 11, 1996.

58. Cohn, R.L., Gasek, N.S., Kuchel, G.A., and Xu, M. (2023). The heterogeneity of cellular senescence: insights at the single-cell level. Trends Cell Biol. 33, 9–17.

59. Grosse, L., Wagner, N., Emelyanov, A., Molina, C., Lacas-Gervais, S., Wagner, K.D., and Bulavin, D.V. (2020). Defined p16 high senescent cell types are indispensable for mouse healthspan. Cell Metabol. 32, 87–99.e6.

60. Liu, J., Ding, Y., Liu, Z., and Liang, X. (2020). Senescence in mesenchymal stem cells: functional alterations, molecular mechanisms, and rejuvenation strategies. Front. Cell Dev. Biol. 8, 258.

61. Lee, S.Y., Fierro, J., Dipasquale, J., Bastian, A., Tran, A.M., Hong, D., Chin, B., Nguyen-Lee, P.J., Mazal, S., Espinal, J., et al. (2022). Engineering human circulating monocytes/macrophages by systemic deliverable gene editing. Front. Immunol. 13, 754557.

62. Attwaters, M. (2022). Targeting senescence in OA. Nat. Rev. Rheumatol. 18, 305.

63. Kondoh, H., and Hara, E. (2022). Targeting p21 for diabetes: another choice of senotherapy. Cell Metabol. 34, 5–7.

64. Lee, Y.N., Wu, Y.J., Lee, H.I., Wang, H.H., Chang, C.Y., Tien, T.Y., Lin, C.F., Su, C.H., and Yeh, H.I. (2021). Ultrasonic microbubble VEGF gene delivery improves angiogenesis of senescent endothelial progenitor cells. Sci. Rep. 11, 13449.

65. Chen, Y., Pu, Q., Ma, Y., Zhang, H., Ye, T., Zhao, C., Huang, X., Ren, Y., Qiao, L., Liu, H.M., et al. (2021). Aging reprograms the hematopoietic-vascular niche to impede regeneration and promote fibrosis. Cell Metabol. 33, 395–410.e4.

66. Gu, Z., Cao, X., Jiang, J., Li, L., Da, Z., Liu, H., and Cheng, C. (2012). Upregulation of p16INK4A promotes cellular senescence of bone marrow-derived mesenchymal stem cells from systemic lupus erythematosus patients. Cell. Signal. 24, 2307–2314.

67. Gu, Z., Jiang, J., Tan, W., Xia, Y., Cao, H., Meng, Y., Da, Z., Liu, H., and Cheng, C. (2013). p53/p21 Pathway involved in mediating cellular senescence of bone marrow-derived mesenchymal stem cells from systemic lupus erythematosus patients. Clin. Dev. Immunol. 2013, 134243.

68. Larijani, B., Foroughi-Heravani, N., Alaei, S., Rezaei-Tavirani, M., Alavi-Moghadam, S., Payab, M., Goodarzi, P., Tayanloo-Beik, A., Aghayan, H.R., and Arjmand, B. (2021). Opportunities and challenges in stem cell aging. Adv. Exp. Med. Biol. 1341, 143–175.

69. Singh, J., Michel, D., Chitanda, J.M., Verrall, R.E., and Badea, I. (2012). Evaluation of cellular uptake and intracellular trafficking as determining factors of gene expression for amino acid-substituted gemini surfactant-based DNA nanoparticles. J. Nanobiotechnol. 10, 7.

70. Caponnetto, F., Manini, I., Skrap, M., Palmai-Pallag, T., Di Loreto, C., Beltrami, A.P., Cesselli, D., and Ferrari, E. (2017). Size-dependent cellular uptake of exosomes. Nanomedicine 13, 1011–1020.

71. Hamsanathan, S., and Gurkar, A.U. (2022). Lipids as regulators of cellular senescence. Front. Physiol. 13, 796850.

72. Xiang, S., Tong, H., Shi, Q., Fernandes, J.C., Jin, T., Dai, K., and Zhang, X. (2012). Uptake mechanisms of non-viral gene delivery. J. Contr. Release 158, 371–378.

73. Vanegas Sáenz, J.R., Tenkumo, T., Kamano, Y., Egusa, H., and Sasaki, K. (2017). Amiloride-enhanced gene transfection of octa-arginine functionalized calcium phosphate nanoparticles. PLoS One 12, e0188347.

74. Nagano, T., Iwasaki, T., Onishi, K., Awai, Y., Terachi, A., Kuwaba, S., Asano, S., Katasho, R., Nagai, K., Nakashima, A., et al. (2021). LY6D-induced macropinocytosis as a survival mechanism of senescent cells. J. Biol. Chem. 296, 100049.

75. Buckley, C.M., and King, J.S. (2017). Drinking problems: mechanisms of macropinosome formation and maturation. FEBS J. 284, 3778–3790.

76. Shin, E.Y., Park, J.H., You, S.T., Lee, C.S., Won, S.Y., Park, J.J., Kim, H.B., Shim, J., Soung, N.K., Lee, O.J., et al. (2020). Integrin-mediated adhesions in regulation of cellular senescence. Sci. Adv. 6, eaay3909.

77. Wheaton, K., Sampsel, K., Boisvert, F.M., Davy, A., Robbins, S., and Riabowol, K. (2001). Loss of functional caveolae during senescence of human fibroblasts. J. Cell. Physiol. 187, 226–235.

78. Ojeda, E., Agirre, M., Villate-Beitia, I., Mashal, M., Puras, G., Zarate, J., and Pedraz, J.L. (2016). Elaboration and physicochemical characterization of niosome-based nioplexes for gene delivery purposes. In Methods in Molecular Biology, Non-viral Gene Delivery Vectors, vol 1445, G. Candiani, ed. (Humana Press Inc.), pp. 63–75.

79. Ayyadevara, V.S.S., and Roh, K.H. (2020). Calcium enhances polyplex-mediated transfection efficiency of plasmid DNA in Jurkat cells. Drug Deliv. 27, 805–815.

80. Ye, Y., Jin, R., Hu, X., Zhuang, J., Xia, W., and Lin, C. (2019). Bioreducible poly(urethane amine)s for robust nucleic acid transfection in stem cells. Biomater. Sci. 7, 3510–3518.

81. Vanegas Sáenz, J.R., Tenkumo, T., Kamano, Y., Egusa, H., and Sasaki, K. (2017). Amiloride-enhanced gene transfection of octa-arginine functionalized calcium phosphate nanoparticles. PLoS One 12, e0188347.

Supplemental information

Development of new non-viral systems

for genetic modification of senescent cells

Junquera López-Seijas, Diego Miranda-Balbuena, Alba Iglesias-Fente, Marta Sacristán-Santos, Natalia Carballo-Pedrares, María C. Arufe, Ana Rey-Rico, and Juan Fafián-Labora
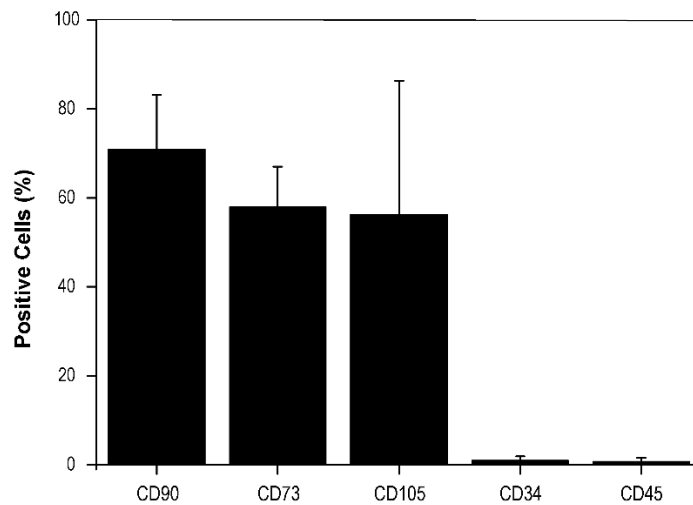
SUPPLEMENTAL INFORMATION

Figure S1. Characterization of UC-MSCs. Histogram of percentage (%) of positive cells for mesenchymal (CD90, CD73 and CD105) and hematopoietic (CD34 and CD45) markers using flow cytometry. Data are shown as mean ± SD.
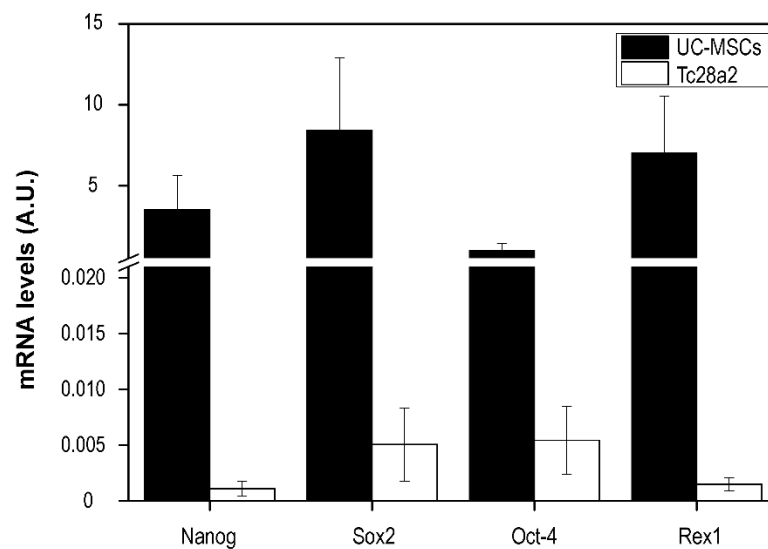
Figure S2. Multipotency profile in UC-MSCs. mRNA levels of undifferentiated stage markers (*NANOG*, *OCT3/4*, *SOX2* and *REX1*) in UC-MSCs and immortalized healthy chondrocytes (TC28a2) using qRT-PCR. Data are shown as mean ± SD.
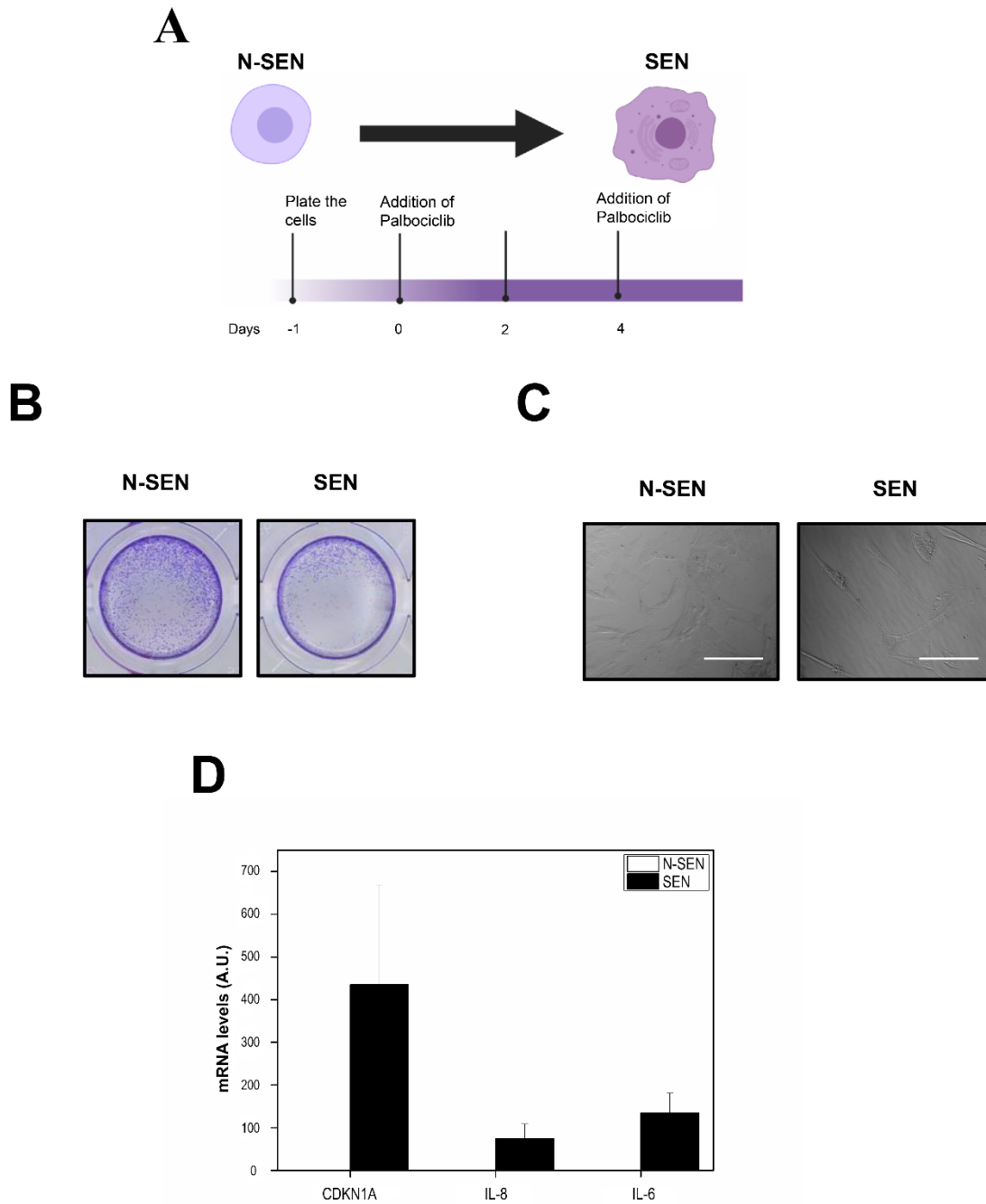
Figure S3. Senescence induction of UC-MSCs. Representative images of crystal violet to evaluate the proliferation capacity of non-senescent (N-SEN) and senescent (SEN) UC-MSCs (**A, B**). Representative images in brightfield of non-senescent (N-SEN) and senescent (SEN) UC-MSCs. Magnification 20X. Scale: 50 µm (**C**). mRNA levels of senescence markers (*CDKN1A*, *IL-8* and *IL-6*) in the non-senescent (N-SEN) and senescent (SEN) UC-MSCs. Data are shown as mean ± SD (**D**).
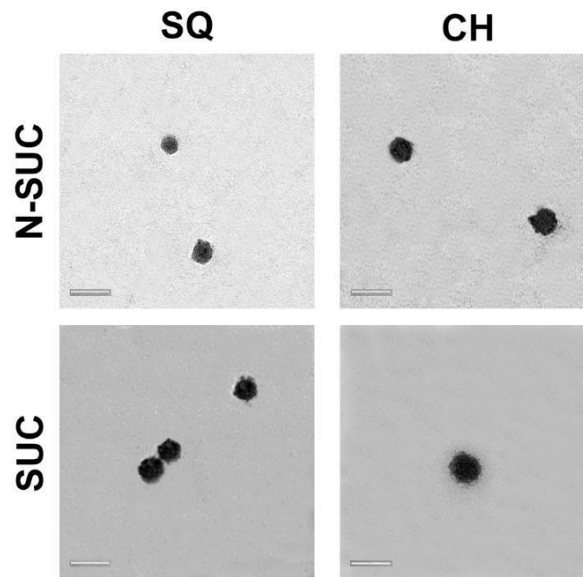
Figure S4. Representative transmission electron microscopy images of squalene (SQ) and cholesterol (CH) niosomes prepared in absence (N-SUC) or presence (SUC) of sucrose. Magnification 100kX. Scale: 200 nm.
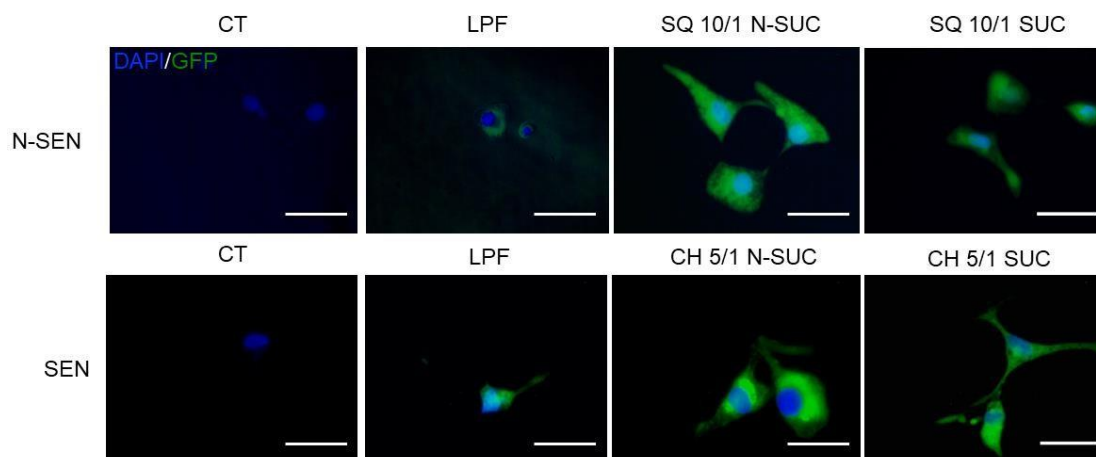

Figure S5. Transfection efficiency of non-senescent and senescent UC-MSCs using nioplexes. Representative DAPI and GFP fluorescence images of non-senescent (N-SEN) and senescent (SEN) UC-MSCs untransfected (CT) or transfected with Lipofectamine (LPF) or with niosome formulations of squalene (SQ) or cholesterol (CH) at 10/1 and 5/1 DOTMA/DNA ratio respectively, in absence (N-SUC) or presence (SUC) of sucrose, for 24 h. Magnification 20X. Scale: 50 µm.
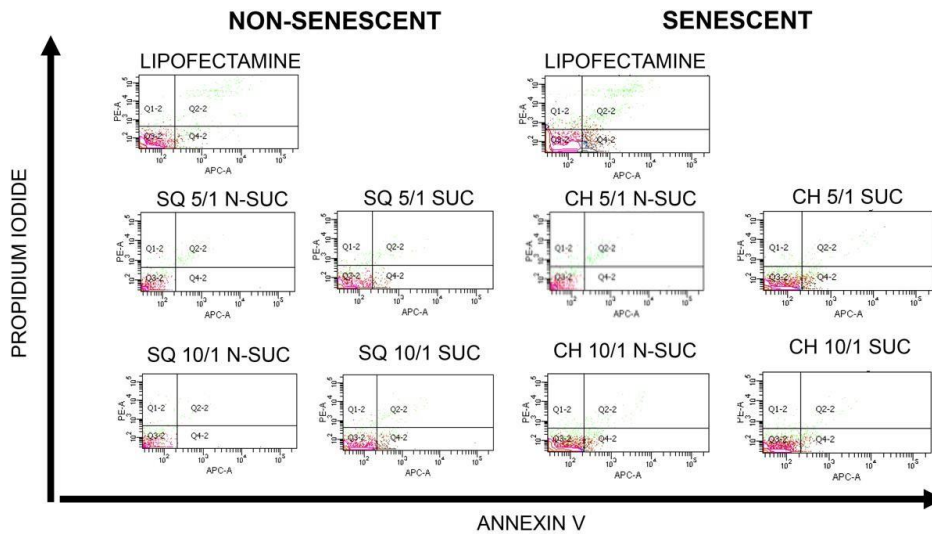
Figure S6. Cytotoxicity after transfection using nioplexes in non-senescent and senescent UC-MSCs. Representative FACs profile showing the PI (PE-A) in front of Annexin V (APC-A) using BD FACSDiva software (BD Science, San Jose, CA, USA) in non-senescent and senescent UC-MSCs transfected with Lipofectamine (LPF) or with niosome formulations of squalene (SQ) or cholesterol (CH) at 5/1 and 10/1 DOTMA/DNA ratios prepared in absence (N-SUC) or presence (SUC) of sucrose for 24 h.
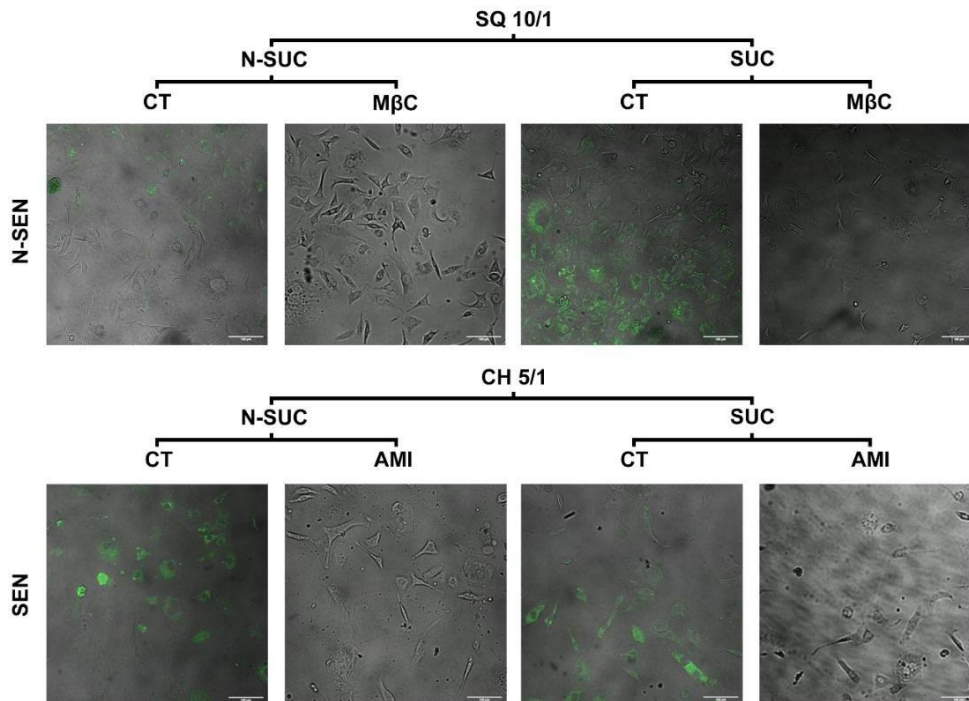

Figure S7. Evaluation of endocytosis pathways by confocal microscopy. Representative confocal GFP fluorescence images of non-senescent (N-SEN) and senescent (SEN) UC-MSCs transfected with LPF or with niosome formulations of squalene (SQ) or cholesterol (CH) at 10/1 and 5/1 DOTMA/DNA ratios respectively, in absence (N-SUC) or presence (SUC) of sucrose. Transfection was performed after preincubation with the endocytosis inhibitors methyl-β-cyclodextrin (MβC) or amiloride (AMI). Control conditions (CT) included cells transfected in absence of inhibitors. Magnification 20X. Scale: 100 μm.
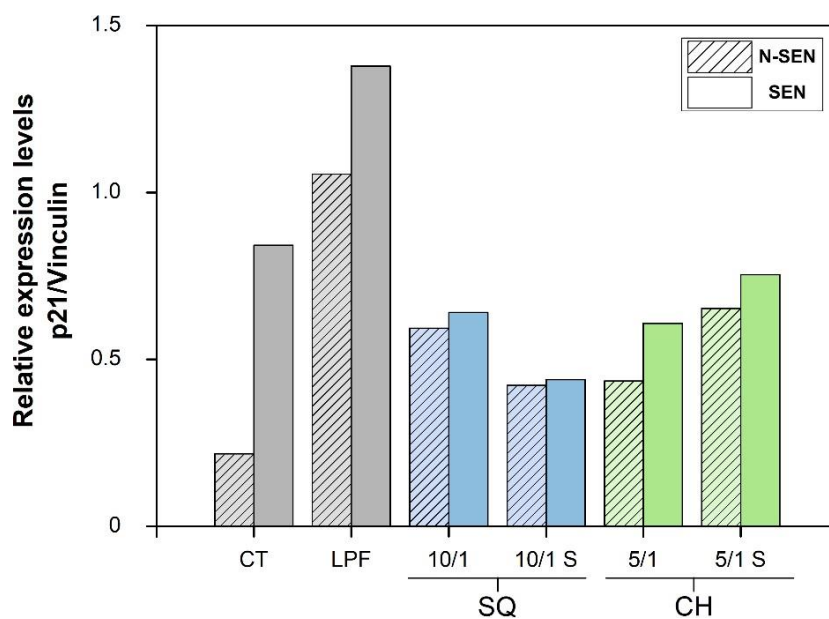
Figure S8. Relative expression levels of senescence markers. Evaluation of senescent phenotype by analyzing p21/vinculin expression ratio in non-senescent (N-SEN) and in senescent (SEN) cells, measured at 72 hours post-transfection using niosome formulations of squalene (SQ) or cholesterol (CH) prepared in absence or presence of sucrose (S) at DOTMA/DNA ratios of 10/1 and 5/1, respectively.

Table S1. Polydispersity index (PDI) of squalene (SQ) or cholesterol (CH) niosome (**A**) and nioplex (**B**) formulations prepared in absence (N-SUC) or presence (SUC) of sucrose.

A

Parameters	Formulation	Niosomes	
	Helper lipid	SQ	CH
PDI	SUC	0.331 ± 0.011	0.312 ± 0.012
	N-SUC	0.331 ± 0.008	0.340 ± 0.022

B

Parameters	Formulation	Nioplexes							
	Helper lipid	SQ				CH			
	DOTMA / DNA ratios	5/1	10/1	15/1	20/1	5/1	10/1	15/1	20/1
PDI	SUC	0.361 ± 0.010	0.328 ± 0.025	0.400 ± 0.032	0.301 ± 0.062	0.256 ± 0.072	0.296 ± 0.041	0.355 ± 0.061	0.394 ± 0.015
	N-SUC	0.225 ± 0.021	0.282 ± 0.027	0.328 ± 0.008	0.304 ± 0.003	0.363 ± 0.024	0.429 ± 0.022	0.300 ± 0.036	0.361± 0.029

Table S2. List of antibodies for FACS and Immunoblot.

Target	Forward	Reverse
CD90	554898	BD PharmigenTM
CD73	561260	BD PharmigenTM
CD105	561443	BD PharmigenTM
CD34	555822	BD PharmigenTM
CD45	555489	BD PharmigenTM
Isotype FICT	556647	BD PharmigenTM
Isotype PE	558595	BD PharmigenTM
Isotype PECy5	550818	BD PharmigenTM
Rabbit Monoclonal p21	ab109520	Abcam
Mouse Monoclonal Anti-Vinculin	Vin-11-5	Sigma-Aldrich
Goat Anti-mouse HRP	P0447	DAKO
Goat Anti-rabbit HRP	P0448	DAKO

Table S3. List of primers sequence for qRT-PCR.

Target	Forward	Reverse
NANOG	ATGCCTCACACGGAGACTGT	AAGTGGGTTGTTTGCCTTTG
SOX2	CTCCGGGACATGATCAGC	GGTAGTGCTGGGACATGTGAA
OCT4	CTCCTGGAGGGCCAGGAATC	ATATACACAGGCCGATGTGG
REX1	CGCAATCGCTTGTCCTCAGAGT	GCTCTCAACGAACGCTTTCCCA
CDKN1A (p21CIP)	CCAGTCCATTTGATCAGCGG	ACATCTTTCTCCCGGGTCTG
IL-8	GAGTGGACCACACTGCGCCA	TCCACAACCCTCTGCACCCAGT
IL-6	CCAGGAGCCCAGCTATGAAC	CCCAGGGAGAAGGCAACTG
ACTB	AGAGCTACGAGCTGCCTGAC	GGATGCCACAGGACTCCA